THE POTENTIAL FOR ACTIVATED BIOCHAR TO REMOVE WATERBORNE VIRUSES FROM ENVIRONMENTAL WATERS

A Thesis

by

JAMES DAVID FLOREY JR.

Submitted to the Office of Graduate Studies of
Texas A&M University
in partial fulfillment of the requirements for the degree of

MASTER OF SCIENCE

May 2012

Major Subject: Soil Science

The Potential for Activated Biochar to Remove Waterborne Viruses from Environmental Waters

THE POTENTIAL FOR ACTIVATED BIOCHAR TO REMOVE WATERBORNE VIRUSES FROM ENVIRONMENTAL WATERS

A Thesis

by

JAMES DAVID FLOREY JR.

Submitted to the Office of Graduate Studies of
Texas A&M University
in partial fulfillment of the requirements for the degree of

MASTER OF SCIENCE

Approved by:

Chair of Committee,	Terry Gentry
Committee Members,	Youjun Deng
	Suresh Pillai
Head of Department,	David Baltensperger

May 2012

Major Subject: Soil Science

ABSTRACT

The Potential for Activated Biochar to Remove Waterborne Viruses from Environmental Waters. (May 2012)

James David Florey Jr., B.S., Texas A&M University

Chair of Advisory Committee: Dr. Terry Gentry

The need for clean potable water and sustainable energy are two current and pressing issues with implications affecting the global population. Renewed interests in alternative energy have prompted researchers to investigate the full capacity of biofuels. These interests have led to not only the examination of current method limitations, but also to the investigation of new conversion methods. One promising method for bioenergy production is pyrolysis of lignocellulosic feedstocks. Through pyrolysis, a single crop may produce ethanol, bio-oil, and/or gaseous energy (syngas). The remaining solid phase product is a black carbon dubbed 'biochar'.

In the current study, biochar was used as a both an unamended sorbent and a precursor to form powdered activated carbons (PACs) capable of removing waterborne viruses. Biochar was activated with KOH, $ZnCl_2$, and H_3PO_4 and analyzed using the Brunauer, Emmett and Teller (BET) method, a combination of Kjeldahl digest and ICP-MS, and scanning electron microscopy (SEM). Sorbents were tested in batch studies using phosphate buffered saline (PBS), surface water, and groundwater. Bacteriophages MS2 and ΦX174 served as viral surrogates.

All activation treatments significantly increased surface area, up to 1495.5 m^2/g (KOH-activated). While the non-activated biochar was not effective in virus removal, the KOH-activated PAC had tremendous removal in the PBS/MS2 batch (mean 98.7% removal, up to 6.2×10^9 particles/mL, as compared to the Darco® S-51: 82.3%).

As evidenced by this study, sorption efficiency will be governed by viral species, carbon type and concentration, and water quality. The results of this study indicate that biochar can serve as a precursor for a highly porous and effective PAC, capable of removing waterborne viruses from environmental waters.

DEDICATION

To He who provides my life's direction. Though I have not always chosen the path or predicted its destination, I need only to keep moving and have faith that His plan is infinitely more perfect than my own. And for my daughter, Malia, who continually provides me with the motivation I could never hope to supply myself.

ACKNOWLEDGEMENTS

I gratefully acknowledge The Department of Soil and Crop Sciences and AgriLIFE Research for funding my studies and the Texas Water Resources Institute for awarding me with the Mills Scholarship.

I'd like to thank my advisor, Dr. Terry Gentry, for the opportunity and counsel and the entire Soil and Aquatic Microbiology Laboratory for their knowledge and assistance. Truly, it takes a village.

I'd like to thank Dr. Jacqueline Aitkenhead-Peterson and Nina Stanley of the Nutrient and Water Analysis Research Laboratory for their assistance with the water sample analysis, Dr. Youjun Deng for his time at the MIC, Alicia Marroquin-Cardona of Toxicology for her help with the BET analysis, and Dr. Don Vietor for the use of his lab.

I must, again, acknowledge the Department of Soil and Crop Sciences of Texas A&M University for providing me with academic and employment opportunities, endless counsel and recommendations from numerous faculty and staff members, and the chance to competitively represent the university. Any future successes I may realize must surely, in some way, be attributed to this department, which has done so much for me.

Lastly, I'd like to thank my support network of family and friends who never had any doubts, whatsoever, in my ability to fulfill the necessary obligations leading to the completion of my degree, despite having positively no idea what those requirements consisted of. Thank you.

TABLE OF CONTENTS

Page

Page

LIST OF FIGURES

Page

Page

LIST OF TABLES

Page

Page

1. INTRODUCTION

The current global needs for alternative energy production have led to renewed interests in biofuels. Biofuel production has, in turn, prompted researchers to address the issue of balancing the energy equation. Often, biofuel production stems from the conversion of agronomic crops to liquid energy products. This process, however, requires inputs that limit net energy production. It is therefore imperative to make this process as efficient as possible. There are two ways to accomplish this: 1) Limit the energy inputs, or 2) Maximize the energy outputs. While the former can be dependent on a number of factors, the latter may be addressed by a method known as pyrolysis.

1.1 Pyrolysis

Pyrolysis is one of the main bioconversion methods currently being developed for the production of biofuels and related bioproducts from various biomass feedstocks. The word "pyrolysis" is derived from the Greek words "pyro", meaning fire, and "lysis", to break down or reduce to constituents (Verheijen et al., 2009). Pyrolysis is a process by which plant biomass is subjected to elevated temperatures in the absence of oxygen, typically in an inert atmosphere such as nitrogen or carbon dioxide. The duration of, and feedstock for, the process can be altered to produce varying relative amounts of

---

This thesis follows the style of the Journal of Environmental Quality.

the three-phase final products: solid (charcoal), liquid (oil), and gas (known as synthesis gas or 'syngas') (Verheijen, 2009; Yaman, 2004). Pyrolysis can either be used independently or combined with other conversion methods such as fermentation. For example, through biomass pyrolysis, a single crop, sugar cane, may be capable of producing three different energy products: ethanol (from the sugar extract of crushed cane), bio-oil, and gaseous energy products (methane, ethane, propane) (Asadullah et al., 2007). While this is encouraging, as it pertains to efficient energy capture, it does not address the need to dispose of, or apply, the resulting charcoal, termed "biochar".

1.2 Biochar

Biochar is a heterogeneous black carbon remnant of plant biomass pyrolysis. The properties and specific constituents of biochar are dependent on the feedstocks and conditions of pyrolysis from which it was created. It can contain significant amounts of oils, tars, salts, metals, ash, and aromatic compounds. While biochar research is a relatively new field, there have already been many proposed applications.

1.2.1 Biochar Application

It has been suggested that biochar incorporation into soil is advantageous on many fronts. Laird et al. (2010) found that biochar added to soil columns acted as a buffer against increases in soil bulk density. Additionally, the authors found that biochar increased soil water retention, specific surface area, and cation exchange capacity. Major et al. (2010) found that biochar-amended soils have increased availability of

calcium and magnesium, which were originally limiting for plant growth in the native soil. This increase was illustrated by maize grain yield and verified by increased Ca and Mg in maize plant tissue. It has also been suggested that biochar additions to soil could enhance biological nitrogen fixation by *Rhizobium* in common beans (*Phaseolus vulgaris* L.) (Rondon et al., 2007). Indeed, there seems to be agreement that biochar amendment generally leads to enhanced microbial activity (Elad et al., 2010; Graber et al., 2010; Laird et al., 2009); however, in some instances, a measurable *decline* in activity has been reported (Van Zwieten et al., 2010). The effects of biochar incorporation on earthworm survival have been studied and, in one instance, found to be both beneficial and detrimental (Liesch et al., 2010). Some suggest that biochar incorporation has great potential for climate change mitigation and carbon sequestration (Lehmann, 2007a; Lehmann, 2007b; Lehmann et al., 2006). Because black carbons, like biochar, persist in the soil longer than other forms of carbon, soil incorporation has been proposed as a potential method for carbon sequestration. This idea has often been related to the "terra preta" soils of the Amazon Basin (Lehmann et al., 2006) which contain large amounts of black carbon thought to have been applied hundreds of thousands of years ago. Such dark, carbon rich soils are an anomaly of the region and represent the potential of a long term C-sink.

While some of these potential benefits have been contradicted by research, others have yet to be roundly studied and may prove to be subject for debate. Whatever the results, one thing is certain, biochar applications are ever evolving.

1.3 Water

1.3.1 Water Availability

The need for clean potable drinking water is, like energy production, a currently pressing issue. As the global population continues to swell, reservoirs and aquifers will continue to shrink under what is already a significant strain. Current global population estimates are 6.9 billion with that number expected to reach 9 billion by 2044 (United States Census Bureau, 2011). One needn't look beyond the Texas borders for the issue of water shortage to be realized. Mandatory water restrictions were already in place for 158 community water systems as of June 2011, by July that number had doubled (TCEQ, 2011). With most of the state listed as being under "exceptional" drought, the most severe rating given under TCEQ's drought severity index, water shortages will likely exert more influence on an already strained system. Despite these facts, here in the U.S., we often take for granted the privilege of readily accessible drinking and irrigation water.

1.3.2 Water Quality

In developing nations, water scarcity is not the only concern. Water *contamination* is still an existing issue, having dire consequences. Examples of common microbial contaminants include protozoa: *Cryptosporidium parvum* (causing Cryptosporidiosis), *Entamoeba histolytica* (Amebiasis); bacteria: *Vibrio cholerae* (Cholera), *Salmonella typhi* (Typhoid fever), *Escherichia coli* O157:H7 (Hemorrhagic diarrhea); and viruses: Hepatitis A virus (Hepatitis), Poliovirus (Polio), Norovirus (Viral

Gastroenteritis). In addition, waterborne disease can commonly be characterized by gastrointestinal illness. If left untreated, gastrointestinal illness can lead to death from dehydration, in some cases. Poverty-stricken nations and, in particular, children are most affected. Per The United Nation's Children's Fund (UNICEF) website:

- In 2002, one in six people had no access to safe water
- ~4500 children die each day from unsafe water and lack of proper sanitation
- >90% of deaths from diarrheal disease occur in children <5 years of age
- Children born in the U.S. or Europe are 520 times less likely to die of diarrheal disease than a sub-Saharan infant (UNICEF, 2006)

Though not subject to the considerable risk posed in developing nations, water quality challenges are still a current issue in the U.S. The populations most sensitive to microbial contaminants include the elderly, the very young (as noted above), and the immunocompromised (those undergoing immunosuppressive therapy, pregnant women, and those living with immune system disease such as AIDS). These populations are not only more likely to become infected, but are also more likely to experience symptoms of greater severity or even death (Reynolds et al., 2008). Indeed, this was the case in the largest waterborne disease outbreak in U.S. history, occurring in Milwaukee, WI, wherein an estimated 403,000 people became infected with cryptosporidiosis. The Milwaukee outbreak resulted in 54 deaths, 85% of which were also attributed to complications from AIDS (Craun et al., 2006).

1.3.2.1 The Challenges of Viral Contaminants

While *Cryptosporidium* could be determined to be the causative agent of the Milwaukee outbreak, since 1941 the largest portion of waterborne diseases outbreaks has an unidentified cause. As viruses are the generally require the most sophisticated methods to detect, it stands to reason that a number of these cases may, in the future, prove to be of viral origin. Of the microbiological contaminants currently listed on the United States Environmental Protection Agency's most recent Contaminant Candidate List, two viruses (*Adenovirus* and Hepatitis A virus) and two viral genera (*Enterovirus* and *Calicivirus*) were included, with *Adenovirus* and *Enterovirus* being recent additions (USEPA, 2009).

Viral contaminants pose unique challenges unrealized by bacterial and protozoan contaminants. Protozoa are generally large enough to be removed via filtration and many bacteria can be inactivated by chlorination. These techniques, however, are often not as effective in treating viral contaminants. Viruses can be orders of magnitude smaller than both protozoa and bacterial cells making standard methods of filtration impractical. Efficacy of disinfection via chlorination is often defined in terms of *Ct* value (where C = concentration of disinfectant, often mg/L; and t = contact time, expressed in minutes). The *Ct* value of *E. coli*, for example, is 0.04 mg/L/min, whereas Poliovirus exhibits a *Ct* value of 1.7mg/L/min (Bitton, 2005). Viruses are also generally thought to persist longer in aqueous environments than their bacterial counterparts (Bosch, 1998). Protection from disinfectants can, for microorganisms, come in the form

of water particulates. Microbes may be protected or shielded from disinfectants through sorption or encapsulation by particulates found in the water complex. More protection is therefore given to smaller organisms, thus favoring viruses. Given the disinfection challenges posed by viral pathogens, it is paramount to develop methods for removing/inactivating viral pathogens found in the water environment. One such method is sorption by activated carbon.

1.4 Activated Carbon

As defined by Dr. Slavoj Cerny, activated carbon is, "…a porous carbonaceous material, prepared by carbonizing and activating organic substances of mainly biological origin. Its most important property is a very large adsorptive capacity, which is primarily due to a highly developed porous structure," (Cerny, 1964). Activated carbon has, in the past, been produced form a number of agricultural wastes, including various nut shells, sugarcane bagasse, corn cobs, pine cones, fruit stones, grasses, and straw (Ioannidou and Zabaniotou, 2007). It can be produced physically, usually with steam, chemically, with some of the most common compounds being $ZnCl_2$, KOH, and H_3PO_4, or with a combination of both physical and chemical activation.

Recently, and likely due to increased interest in energy from pyrolysis, carbon activation has incorporated the use of biochars. Azargohar and Dalai (2006 & 2008) produced activated carbon, with both steam and KOH, from the char of spruce. Their findings concluded that an active carbon with a Brunauer, Emmett, and Teller (BET) surface area of 1578 m^2/g could be produced from biochar. Comparatively, the

industrially produced activated carbon used in this study was determined to have a BET surface area of ~541 m^2/g.

1.4.1 Applications of Activated Carbon

In the past, activated carbons have had a range of applications. They are commonly used in air filters and industrial gas masks to remove malodorous products or potentially harmful aerosols. The food and beverage industry has used activated carbons to remove unacceptable colors or tastes. In water treatment, activated carbons are commonly used to remove dissolved organics, harmful metals like Hg, Pb, or Cu, and byproducts of chemical water treatment, like trihalomethanes. Though not as commonly applied, the effects of activated carbon on virus retention have been previously studied. As far back as 1975, Poliovirus was used in batch studies to determine the effects of an active carbon in secondary effluent (Gerba et al., 1975). The authors concluded that virus removal was highly dependent on pH as well as the concentration of organics in wastewater. Seo et al. (1996) used a powdered activated carbon (PAC) produced by Toyo to remove the F^+ (F-specific)-RNA coliphage Qβ from synthetic secondary sewage effluent. Coliphage Qβ was, according to Seo, chosen due to its structural resemblance to human-pathogenic viruses. Qβ, however, poses no threat to human health. This study showed the PAC to be 99.999% effective in removing the coliphage, at 0.55 g PAC/L.

1.5 Coliphages as Surrogates for and Indicators of Waterborne Viral Pathogens

As demonstrated in the above study, coliphages are commonly used as indicators of fecal/viral contamination since they are enteric viruses and therefore present where one might expect to find enterobacteria, specifically *E. coli*, and waterborne viral pathogens, like Poliovirus, Hepatitis A and E viruses, and Norovirus. This sentiment was echoed by Bosch (1998) who stated somatic coliphages, F-specific bacteriophages, and *Bacteroides fragilis* bacteriophages would make suitable candidates for organisms indicative of pathogenic viral presence. Not only are they morphologically similar to pathogenic viruses, but they also exhibit similar behavior in aquatic environments. They are generally present in considerable numbers in polluted waters and their relatively high degree of resistance to disinfectants has made them attractive model organisms. These bacteriophages are not harmful to humans, and, because they rely on readily cultured bacterial hosts, they are easy to detect and quantify in the lab with simple and inexpensive methods. Two such phages, MS2 (an F-specific bacteriophage) and ΦX174 (a somatic coliphage), were used in this research project.

1.5.1 The Bacteriophages MS2 and ΦX174

The bacteriophages MS2 and ΦX174 are similar in size and morphology to known pathogenic viruses of fecal origin; and yet, they maintain significant differences. MS2 has an ssRNA genome and a diameter of 24-26 nm (Golmohammadi et al., 1993), while ΦX174 has an ssDNA (circular) genome and a diameter of 25-27nm (ICTVdB, 2006; McKenna et al., 1992). Both are non-enveloped; but, while MS2 has a T=3

triangulation number, and an isoelectric point (IEP) of 3.9 (Overby et al., 1966), ΦX174 has a T=1 triangulation and an IEP of 6.6 (Chattopadhyay and Puls, 1999). Additionally, ΦX174 exhibits 'spike' proteins at each of the 12 pentameric vertices in its icosahedral capsid (ICTVdB, 2006; Ilag et al., 1994).

1.6 Study Objectives

It is the purpose of this study to merge the highly significant and current global issues discussed above: 1) the need for alternative energy sources and 2) the need for clean, potable water. In a general sense, this objective was to be accomplished by using biochar, or products created using biochar as a precursor, to remove waterborne viruses with the bacteriophages MS2 and ΦX174 serving as viral surrogates. Specifically, for this goal to be realized, the following objectives were selected:

1. Determine the potential of a non-activated biochar for removing waterborne viruses.
2. Determine/select activation parameters for said biochar and compare the ability of three different chemical activating agents to produce a PAC capable of removing/inactivating waterborne viruses.
3. Physically and chemically characterize the biochar and resulting activated carbon produced from the three chemical treatments.
4. Determine the efficiency of the three PACs to remove/inactivate viral pathogens from various aqueous matrices.

2. METHODS

2.1 Biochar

The biochar used in this study was generously donated by the lab of Dr. Don Vietor, Soil and Crop Sciences Department, Texas A&M University (TAMU). The material was produced through pyrolysis of corn stover at 550 °C through an auger-fed, fixed-bed pyrolyzer. Dinitrogen gas was used to purge the system, prior to pyrolysis, in order to remove any O_2. The biochar was then ground for 30 seconds in a ring and puck grinder and passed through a 200 mesh sieve.

2.2 Bacteriophages

Bacteriophages MS2 (ATCC #15597-B1) and ΦX174 (ATCC #13706-B1), and their respective host strains *E. coli* F^+ amp (ATCC #15597) and *E. coli* C (ATCC #13706), were obtained from the American Type Culture Collection (ATCC). The two phages were chosen as they are similar in size and morphology to known pathogenic viruses of fecal origin (Bosch, 1998; Seo et al., 1996). The phages and hosts were propagated according to Standard Methods for the Examination of Water and Wastewater, Method 9224 B & C (American Water Works Association, 2005) with the following modifications: LB Broth was substituted for the tryptone, yeast extract, and NaCl requirements of the media described in Method 9224. Additionally, both 30 mL phage/host suspensions were brought to 1M NaCl before being chilled at 4 °C and

centrifuged for 10 minutes at 4000 X g. The purpose of these additional steps was to aid in phage separation/dispersal as well as filtration. The supernatant was then collected and passed through a 1.5% beef extract-treated Supor® 200, 47 mm, 0.20 µm filter (Pall Life Sciences, Port Washington, NY, USA). The filtrate was serially diluted (10-fold) with phosphate buffered saline (PBS) pH 7.4 ± 0.2. Dilutions were plated in triplicate, via methods described in Methods 9224 B & C, in order to determine phage titer.

2.3 Batch Matrices

Matrices for batch assays consisted of the following: PBS, pH 7.4 ±0.2; an untreated surface water sample, and an untreated groundwater sample.

2.3.1 Phosphate Buffered Saline (PBS)

The PBS was made according to United States Environmental Protection Agency (USEPA) Method 1603 (USEPA, 2002) and consisted of the following:

Monosodium phosphate (NaH_2PO_4)	0.58 g
Disodium phosphate (Na_2HPO_4)	2.5 g
Sodium chloride (NaCl)	8.5 g
Reagent-grade water	1.0 L

The solid ingredients were dissolved in the water with the use of a magnetic stir plate and autoclaved at 121 °C for 20 minutes. Final pH was 7.4 ± 0.2.

2.3.2 Surface Water

The surface water sample was collected from Wolf Pen Creek in Wolf Pen Park, a local, urban stream system in College Station, Texas 77840. The sample was collected in an 18 liter carboy. The collection site was within the park, south of Holleman Drive East and east of Dartmouth Street.

2.3.3 Groundwater

The groundwater sample was collected with the aid of Texas A&M University Water & Environmental Services from TAMU Water Production Well #7 (WPW7) located at 6055 Fountain Switch Rd. Bryan, TX 77807. The sample was pumped directly into a 38 liter carboy at a temperature of 42+ °C. The well pumps from the Carrizo-Wilcox Simsboro Sands aquifer at a depth nearing 3200 feet.

2.3.4 Surface and Ground Water Characterization

The environmental water samples were analyzed via the following methods:

2.3.4.1 pH and Conductivity

Environmental water pH was determined using a Beckman 255 pH meter. Conductivity was measured using an Omega model CDH-5021 conductivity tester. Conductivity was reported as µS/cm.

2.3.4.2 Anions/Cations

Anions (F^-, Cl^-, and SO_4^{2-}) were quantified using gradient ion chromatography with a Dionex IC 2000 (Dionex Corp. Sunnyvale, CA, USA). The analytical column was an Ionpak AS20 (4 x 250 mm) and the guard column was an Ionpak AG20 (4 x 50 mm). The eluent was 35 mM KOH at a flow rate of 1.0 mL/min and an injection volume of 25 µL. Cations (Na^+, K^+, Mg^{2+}, and Ca^{2+}) were quantified using isocratic ion chromatography with a Dionex IC 1000. An Ionpac CS12A (5 x 250 mm) and Ionpac CG12A (5 x 50 mm) were used for analytical and guard columns, respectively. The eluent was 20 mM methanosulfonic acid at a flow rate of 1.0 mL/min and an injection volume of 258 µL.

2.3.4.3 NO_3-N, NH_4-N, PO_4-P

Colorimetric methods were used to determine NO_3-N, NH_4-N, and PO_4-P using USEPA Methods 353.2 (USEPA, 1993a), 350.1 (USEPA, 1993b), and 365.1 (USEPA, 1993c), respectively. All colorimetric analyses were conducted with the Westco Scientific SmartChem Discrete Analyzer (Westco Scientific Instruments Inc. Brookfield, CT, USA).

2.3.4.4 Non-Purgeable Organic Carbon (NPOC) and Total Dissolved Nitrogen (TDN)

Non-purgeable organic carbon (NPOC) and total dissolved nitrogen (TDN) were quantified using high temperature platinum-catalyzed combustion on a Shimadzu TOC-V_{CSH} with a TNM-1 total measuring unit (Shimadzu Corp. Houston, TX, USA). The

NPOC quantification included acidification (250 µL of 2M HCL) and sparging (4 min) of the sample with carbon-free air to remove volatile carbon and was measured with nondispersive infrared sensor detection (NDIR) and TDN by chemiluminescence detection.

2.3.4.5 Determination of *E. coli* Concentration in Surface Water

The concentration of *E. coli* within the surface water sample was determined in accordance with USEPA Method 1603: *Escherichia coli* (*E. coli*) in Water by Membrane Filtration Using Modified membrane – Thermotolerant *Escherichia coli* Agar (Modified mTEC) (2002).

2.4 Carbon Activation

Based on review of the available literature, it was determined that pore size may be critical for the efficiency of active carbon sorption. Because phage particles are substantially larger than the molecular compounds generally sorbed by PACs, the activation parameters were specifically selected for the creation of larger pores. To accomplish this, parameters were used that resulted in pore destruction, and the creation fewer pores of greater diameter (Azargohar and Dalai, 2008) thus allowing for sorption of the phage particles. With these goals in mind, the following parameters were used:

- Maximum temperature: 850 °C
- Duration at maximum temperature: 1.5 hours

- Heating (ramp) rate: 5 °C/minute
- Chemical activating agent to biochar ratio: 2:1, by weight basis
- Atmosphere: nitrogen gas (N_2)
- N_2 flow rate: 300 mL/minute
- Chemical activating agents: KOH, $ZnCl_2$, H_3PO_4

A 40-gram aliquot of biochar was thoroughly mixed with the respective chemical agent for two hours after which the suspension was allowed to dry in an oven at 120 °C. The dried material was then ground with a mortar and pestle and passed through a 1-mm sieve. The biochar was then loaded, on stainless steel boats, into a tubular furnace reactor with a length of 60.96 cm and a diameter of 2.54 cm and activated via the aforementioned parameters. The activated biochar was washed with distilled water, mixed with 0.1M HCl, and rinsed again with distilled water until the suspension pH ranged from 6-7. A Whatman 540 (hardened-ashless, 8 µm pore) filter was used to separate the biochar from the aqueous phase between washes. The activated and washed biochar was allowed to dry overnight at 100 °C before being ground with a mortar and pestle and passed through a 200 mesh sieve. The material was thenceforth referred to as PAC.

2.5 Biochar/PAC Characterization

The non-activated biochar and subsequent PACs were analyzed via the following methods:

2.5.1 Surface Area

The surface area of the activated/non-activated biochars was determined using the Brunauer, Emmett, and Teller (BET) method with a Micromeritics® (Micromeritics Instrument Corp., Atlanta, GA, USA) Accelerated Surface Area and Porosity (ASAP) 2020 V3.01E analyzer. Samples were degassed at 300 °C and analyzed using N_2 as an adsorptive. The BET equation was used to calculate surface area as per the manufacturer's instructions.

2.5.2 Imaging

Samples were examined using scanning electron microscopy (SEM), performed at the TAMU Microscopy & Imaging Center. Samples were prepared by suspending a small amount of PAC/biochar in de-ionized water. A standard SEM platform was topped with a double sided adhesive tab onto which a few drops of suspension were placed. The platform was then covered with a watchglass and allowed to dry under a heating lamp. The samples were then coated with a 4.0 nm alloy coating, consisting of Pt and Pd, and viewed with a QUANTA 600FE-SEM (FEI Co. Hillsboro, OR, USA). Backscatter images and EDS spectra were also captured.

2.5.3 Elemental Analysis

Elemental analysis was determined at the Texas AgriLife Extension Service - Soil, Water and Forage Testing Laboratory. Total nitrogen and organic carbon were determined, on a percent basis, by a combustion process (McGeehan and Naylor, 1988).

Total Ca, Cu, Fe, K, Mg, Mn, Na, P, and Zn were determined with inductively coupled plasma (ICP) spectrometry of a nitric acid digest (Havlin and Soltanpour, 1980). Those results were reported on an mg/kg basis.

2.6 Batch Analyses

Batch analyses were conducted in the laboratory using the aforementioned matrices, phages, and biochar/PACs.

2.6.1 Effects of Non-Activated Biochar on MS2 Levels

To determine the effectiveness of non-activated biochar on viral particle removal, 50 mg of untreated, ground, sieved biochar was combined, in a 250 ml Erlenmeyer flask, with 200 mL of PBS and mixed, on a stir plate, for 15 minutes at 380 rpm before being seeded with concentrated MS2. The solution was then mixed for two hours at 380 rpm before being passed through a Supor® 200, 47 mm diameter, 0.20 µm pore-size filter (Pall Life Sciences, Port Washington, NY, USA). The filtrate was assayed for MS2 infectivity according to Method 9224 (American Water Works Association, 2005). Additionally, a baseline batch, containing no biochar, was seeded and assayed to determine basal MS2 infectivity, to which all other treatments were compared. Darco® S-51 PAC (Norit Americas Inc. Marshall, TX, USA), supplied by Norit-Americas, served as the sorbent in the PAC control batch. One non-seeded batch containing only PBS and biochar was also assayed to quantify potential indigenous MS2 particles. These batches were run simultaneously. Each test was replicated at least three times.

2.6.2 Effects of Activated Biochars on MS2 Levels in PBS

The powdered activated carbons from biochar treated with KOH, $ZnCl_2$, and H_3PO_4 were also assayed for sorption, as described above. Five batches: baseline, KOH-PAC, $ZnCl_2$-PAC, H_3PO_4-PAC, and Darco® S-51 PAC were all mixed and processed simultaneously, as described above. Various concentrations of MS2 inoculum, ranging from 1.82×10^4 - 6.25×10^9 particles/mL in the resulting baseline filtrates, were tested in order to optimize treatment efficacy and enable delineation of treatment effects.

2.6.3 Effects of Activated Biochars on MS2 and ΦX174 Levels in a Surface Water Matrix

The effectiveness of the activated biochars in a surface water matrix was also assayed. Collection and characterization of the surface water sample was carried out as described above. Various concentrations/volumes of phage inoculum and surface water concentration were tested in order to optimize treatment efficacy and enable delineation of treatment effects. Based upon these results, subsequent batch trials used 75% surface water. Surface water matrix batches consisted of 50 mg of each PAC and 50 mL of 75% surface water and 25% PBS. These were combined and mixed in a 125 mL Erlenmeyer flask. All other parameters were as described above except that the surface water batches, once mixed, required pre-filtration with a 47 mm diameter, 0.45 µm pore-size Millipore S-PAK™ membrane filter (Millipore Corp. Billerica, MA, USA), prior to finally passing through a Supor® 200, 47 mm diameter, 0.20 µm pore-size filter. This

step was needed as the high levels of solids in the surface water clogged the 0.20 μm filter when used alone. These assays were conducted separately for each phage: MS2 and ΦX174.

2.6.4 Effects of Activated Biochars on MS2 and ΦX174 Levels in a Groundwater Matrix

The effectiveness of the activated biochars in a ground water matrix was also assayed. Collection and characterization of the groundwater sample was carried out as described above. Like surface water matrix batches, groundwater matrix batches consisted of 50 mg of each PAC and 50 mL of groundwater combined and mixed in a 125 mL Erlenmeyer flask. Again, various concentrations/volumes of phage inoculum and groundwater volume were tested; the ground water concentration was 100%. Groundwater batches required no pre-filtration once mixed as they did not contain significant amounts of suspended solids. Otherwise, all parameters were as described above, and each phage, MS2 and ΦX174, were separately tested.

2.7 Mode of Inactivation

To provide evidence supporting the physical removal of viral particles by PACs, extract batches were used as matrices for assays to assess chemical inactivation potential (i.e. to demonstrate that any reduction in viral particles was due to binding by activated biochar and not chemical inactivation). Briefly, all PACs (50 mg) were mixed with 200 mL of PBS as described above with exception: batches were not inoculated until after

phase separation. Batch filtrate for all treatments was collected, inoculated, mixed for an additional 0.5 hours, and assayed for MS2 infectivity, as described above.

Additionally, to determine the potential influence of the activated biochars on solution pH, a Fisher Accument Basic (Fisher Scientific, Pittsburgh, PA, USA) AB 15 pH meter was used to record the initial groundwater pH; then, 10 mg of each PAC was placed in a 16 mm diameter test tube along with 10 mL of the aforementioned groundwater sample. Groundwater was chosen as it was thought to likely have less buffering capacity than the surface water. The concentration of PAC to groundwater represented the same concentration as the surface and groundwater matrix batches. The tubes were then vortexed, covered with test tube caps, and allowed to sit at room temperature for 1.0 hour after which they were vortexed again and allowed to sit for an additional hour. After 2.0 hours at room temperature, the solution pH of each tube was recorded with the aforementioned pH meter.

2.8 Statistical Analysis

Data was collected and reported as PAC/biochar virus removal efficiency. Batch assays were replicated at least three times. Batch filtrates were plated, at minimum, in duplicate with the mean plaque forming units (PFU)/mL being recorded. This data was then compared to the baseline infectivity and interpreted as % removal efficiency. Additionally, all treatments were analyzed via the student's t-test at an alpha of 0.05 for statistical delineation. Data was analyzed using JMP® version 9.0.0 software.

3. RESULTS

3.1 Bacteriophage Propagation

3.1.1 MS2 Propagation

Following propagation, plate count results were compared across time taken to ensure the viability of the MS2 inoculum. As MS2 has previously displayed a susceptibility to osmotic shock, PBS was chosen as the diluent. The resulting titer was determined to be 3.52×10^{12} PFU/mL.

3.1.2 ΦX174 Propagation

Bacteriophage ΦX174 was propagated as described above. The resulting titer was determined to be 2.3×10^{8} PFU/mL.

3.2 Biochar Activation

The results of the total yield from heat treatment of all biochars can be seen in Table 1.

Table 1: Biochar Recovery After Heat-Treatment for All Activation Treatments

Activation Treatment	Mean Recovery (%)	Std. Dev. Of the Mean
KOH	61.4	6.3
$ZnCl_2$	29.3	1.9
H_3PO_4	31.9	2.0

3.2.1 Biochar Activation

Total KOH used for activation was 39.96 g as compared with 20.06 g of ground biochar, mixed in 100 mL of de-ionized water (DI H_2O). As seen in Table 1, mean recovery from heat treatment was 61.43%. It should be noted, however, that some material from the first and second activation trials was spilled and therefore these runs were not used to calculate recovery %. Total activated material subjected to acid/water washing and rinsing was 20.848 g. After washing, rinsing, oven drying, and sieving, the final KOH-activated product was 3.779 g.

Total $ZnCl_2$ used for activation was 40.03 g as compared with 20.00 g of ground biochar, mixed in 100 mL DI H_2O. As seen in Table 1, mean recovery from heat treatment was 29.29%. Total amount of $ZnCl_2$-activated biochar subjected to acid/water washing and rinsing was 10.833 g. Final product totaled 7.872 g.

Activation with H_3PO_4 consisted of 100 mL of diluent containing 40 g H_3PO_4 added to 19.94 g of ground biochar**.** As seen in Table 1, mean recovery from heat treatment was 31.89%. Total amount of H_3PO_4-activated biochar subjected to acid/water washing and rinsing was 7.250 g. Final product totaled 6.022 g.

3.3 Biochar/PAC Characterization

3.3.1 Surface Area

The results of the surface area analysis, as determined by the Brunauer, Emmett, and Teller (BET) method and calculated using the BET formula, are seen in Figure 1. Surface area of the non-activated ground biochar was 3.64 m^2/g. The most dramatic

results were seen in the KOH-activated biochar which produced a PAC with almost three times the surface area of that found in the Darco® S-51 PAC. The next highest value was found in the H_3PO_4-activated biochar, with a surface of area of less than half that of the KOH-activated biochar, followed by the $ZnCl_2$-activated biochar. All PACs produced from biochar resulted in surface area values greater than that of the Darco® S-51 PAC and many times greater than that of the non-activated precursor.

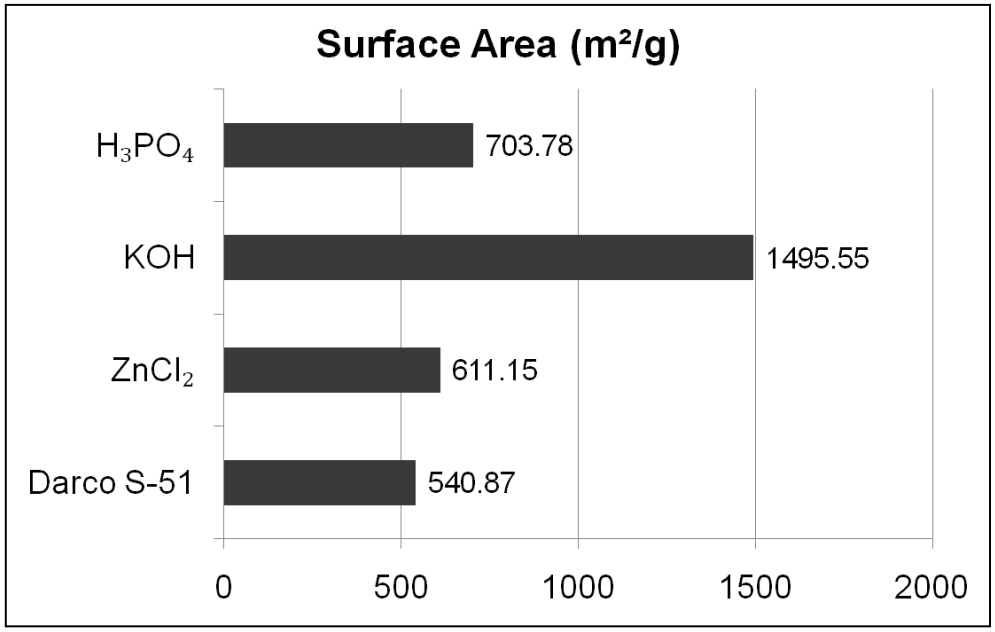

Figure 1: Brunauer, Emmett, and Teller Surface Area of PACs

3.3.2 Elemental Analysis

As indicated by the elemental analysis (Table 2), the activation process altered the relative quantities of measured elements. Chemical treatment also had an effect on the elemental composition as elemental proportion differed amongst the varying

treatments and in comparison to their relative shifts from the non-activated biochar composition. Not surprisingly, PACs resulting from activation with $ZnCl_2$ and H_3PO_4 realized increases in Zn and P, respectively. Such was not the case, however, for KOH-activated biochar which actually contained less relative K than did the H_3PO_4-activated biochar. All treatments resulted in an increase in proportional C, as compared with the non-activated biochar; however, the highest relative C was found in the industrial PAC, Darco® S-51.

3.3.3 Imaging

The following images, along with EDS data, were captured at the Microscopy and Imaging Center of Texas A&M University.

3.3.3.1 Non-Activated Biochar

Figure 2 displays four images of the non-activated biochar. Images A and C represent the same frame at different magnification (4000 and 20000X, respectively) while images B and D represent another frame, also at different magnification (2000 and 8000X, respectively). Comparatively, the material in Figure 2 contains relatively smooth surfaces, lacking the texture and porosity seen in images of activated material.

Table 2: Elemental Analysis of Biochar/PACs as Determined by Kjeldahl Digest/ICP-MS

	Element										
Treatment (Mean of 3 Reps)	**% C**	**% N**	**P g/kg**	**K g/kg**	**Ca g/kg**	**Mg g/kg**	**Na mg/kg**	**Zn mg/kg**	**Fe mg/kg**	**Cu mg/kg**	**Mn mg/kg**
Non – Activated	54.2 ± 0.3	1.5 ± 0.1	1.9 ± 0.1	103.3 ± 7.4	8.5 ± 0.3	3.8 ± 0.3	402.1 ± 84.7	71.7 ± 3.4	714.0 ± 64.1	22.4 ± 0.9	119.8 ± 11.4
KOH – Activated	60.5 ± 0.8	1.94 ± 0.1	1.0 ± 0.06	11.2 ± 0.9	10.5 ± 0.3	4.0 ± 0.2	343.2 ± 256.1	59.6 ± 5.0	941.0 ± 169.5	47.1 ± 1.0	352.1 ± 21.4
$ZnCl_2$ – Activated	72.1 ± 3.8	1.72 ± 0.1	3.3 ± 0.1	5.8 ± 0.6	3.6 ± 0.2	1.5 ± 0.09	498.8 ± 267.2	2358.6 ± 258.9	537.0 ± 35.6	191.4 ± 6.8	701.6 ± 60.9
H_3PO_4 – Activated	51.3 ± 0.1	1.46 ± 0.1	72.6 ± 3.8	14.6 ± 0.7	14.3 ± 0.4	5.1 ± 0.2	802.1 ± 101.6	398.9 ± 8.2	754.7 ± 169.2	205.5 ± 6.5	614.3 ± 28.7
Darco S-51	78.8 ± 0.4	0.93 ± 0.1	0.4 ± 0.01	0.7 ± 0.2	2.1 ± 0.04	0.8 ± 0.2	2016.1 ± 231.0	4.4 ± 0.5	398.8 ± 84.6	31.0 ± 0.6	16.2 ± 4.0

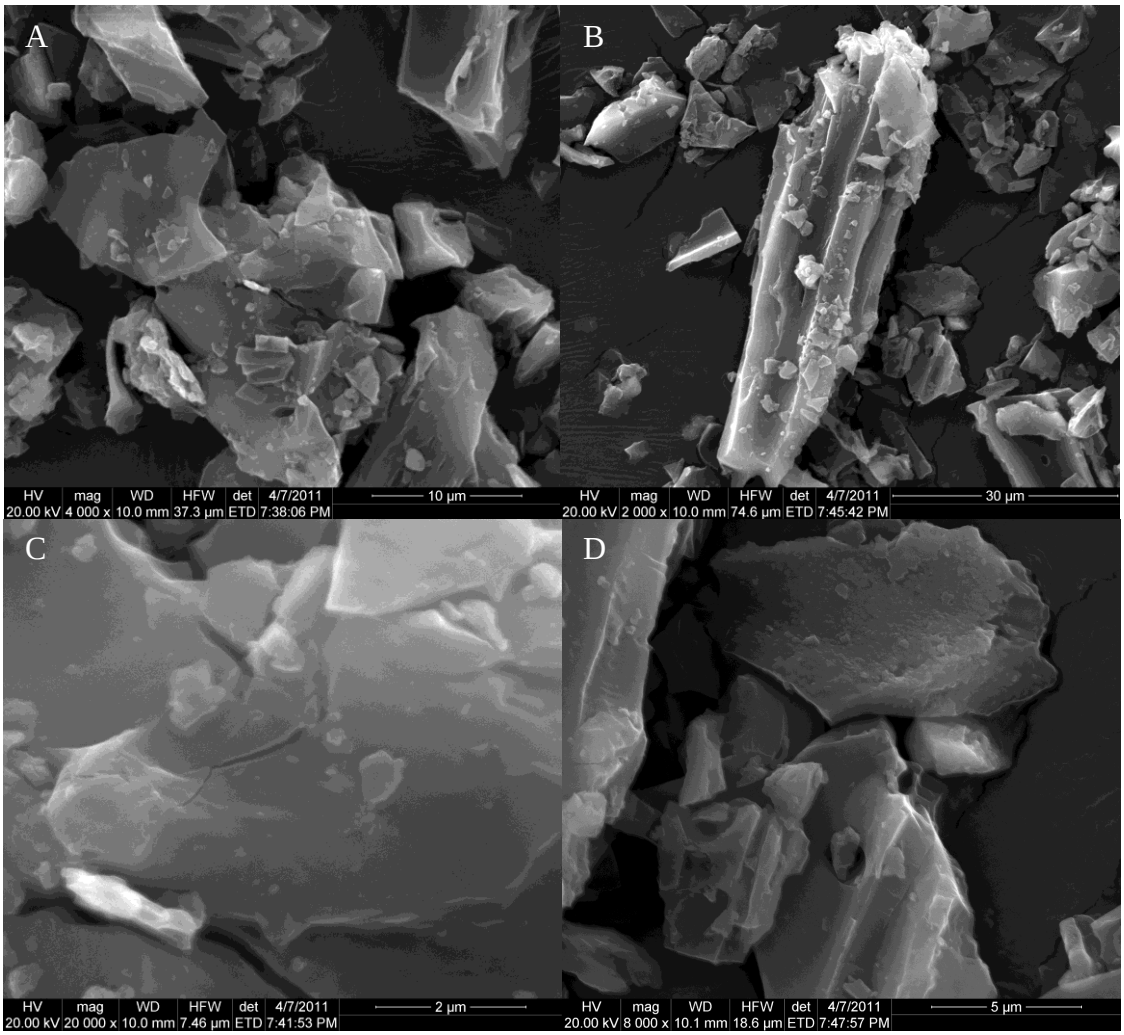

Figure 2: SEM Images of Non-Activated Biochar at A) 4000X Magnification, B) 2000X, C) Image A at 20000X, and D) Image B at 8000X

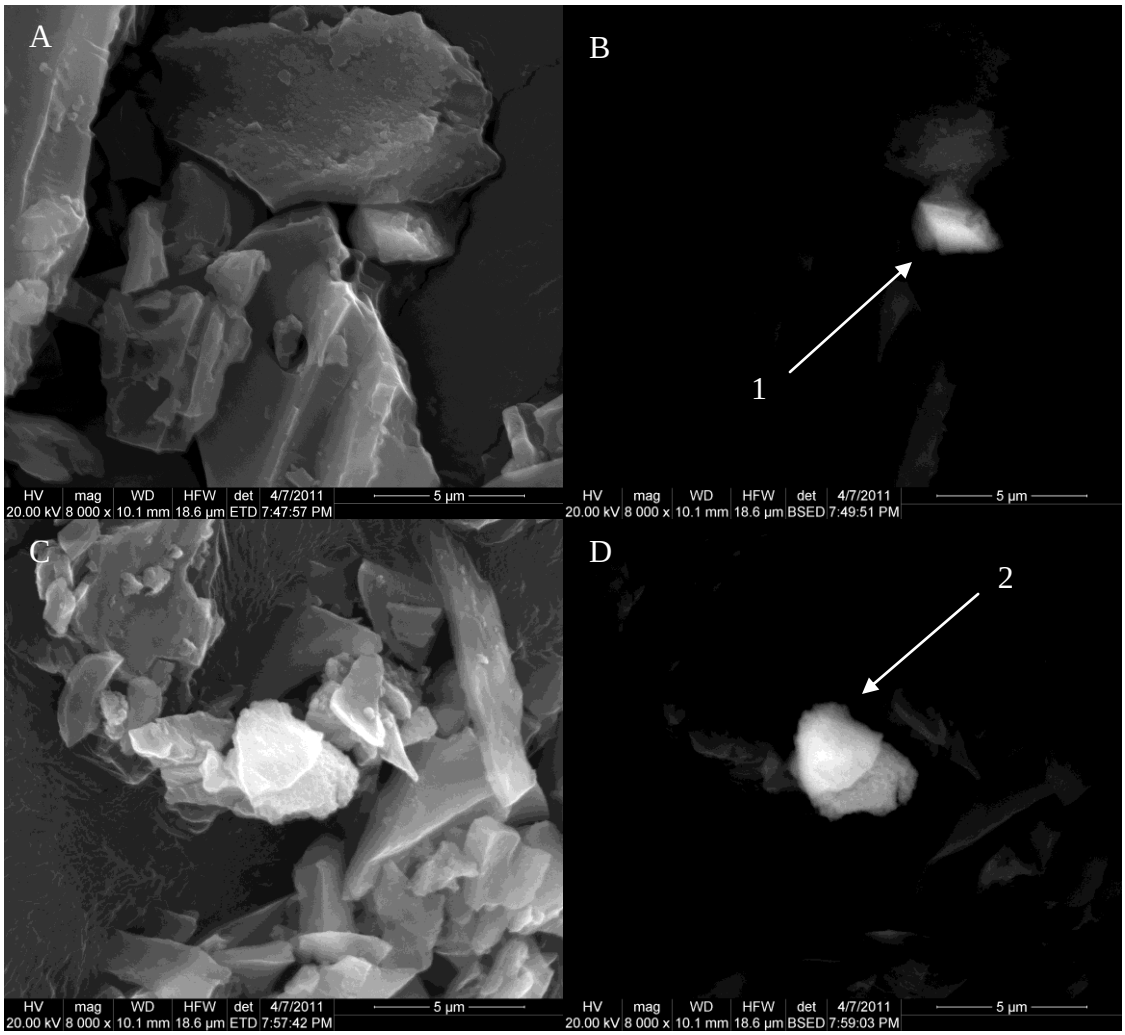

Figure 3: SEM Images of Non-Activated Biochar at A) 8000X, B) Backscatter View of Image A, C) 8000X, and D) Backscatter View of Image C

Figure 3 displays two images of the non-activated biochar at 8000X magnification (image A and C) and their respective backscatter views (B and D, respectively). The backscatter image displays compounds of high density, usually heavy metals and/or metal complexes (points 1 & 2). Figure 4 displays selected points from image A (Figure 3) from which EDS spectra were captured.

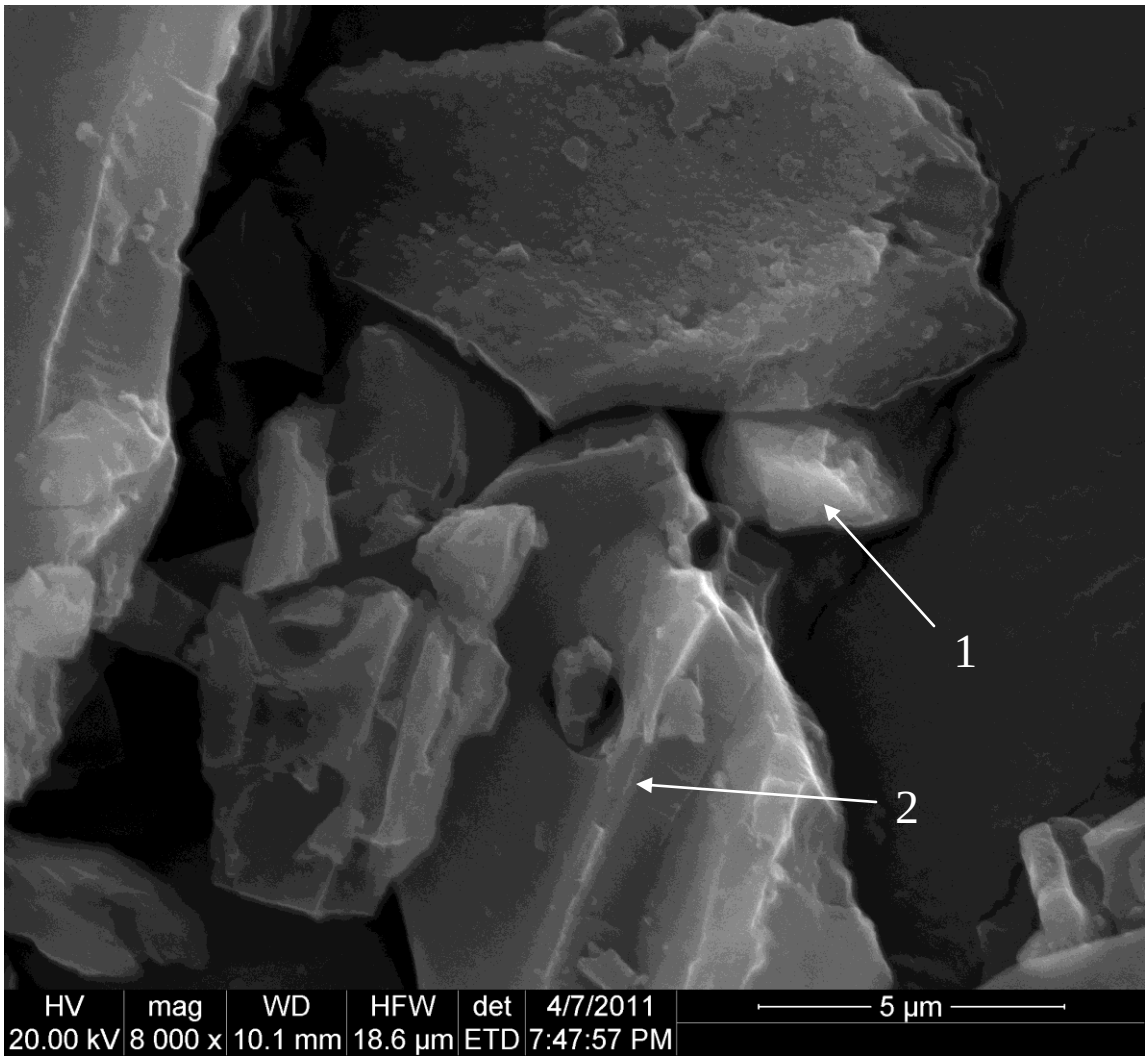

Figure 4: SEM Image of Non-Activated Biochar at 8000X Magnification from Which EDS Spectra Were Taken at Points 1&2

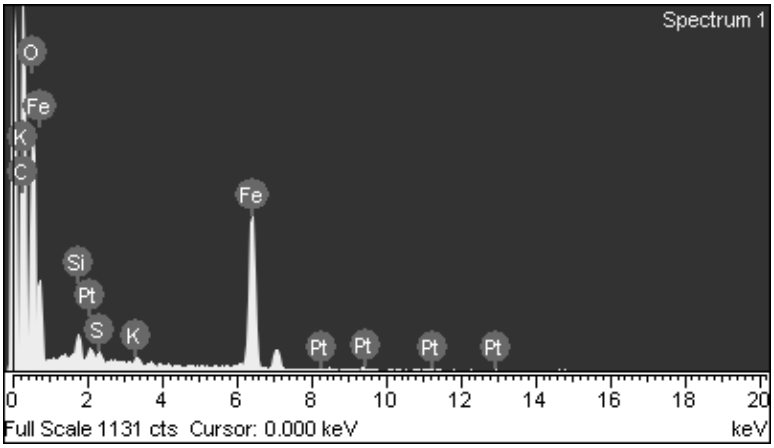

Figure 5: EDS Spectra of Non-Activated Biochar at 8000X Magnification. Point 1, Figure 4

Table 3: Elemental Composition Taken from Spectrum 1 of Figure 4-Non-Activated Biochar at 8000X Magnification

Element	Weight%	Atomic%
C	36.64	60.3
O	19.06	23.54
Si	1.76	1.24
S	0.92	0.57
K	0.86	0.43
Fe	38.74	13.71
Pt	2.02	0.2
Totals	100	

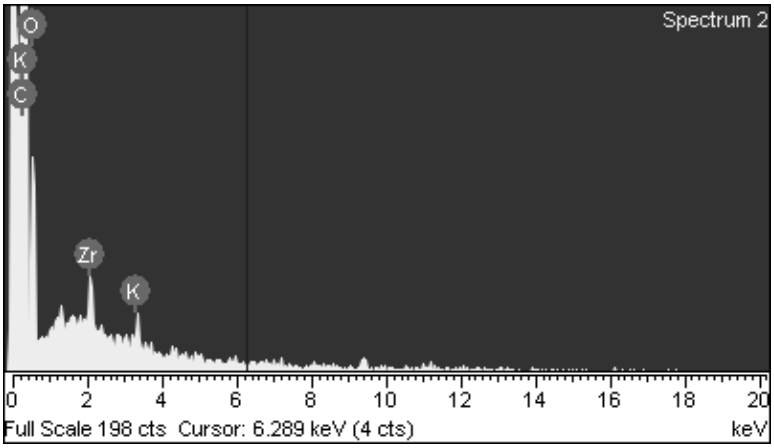

Figure 6: EDS Spectra of Non-Activated Biochar at 8000X Magnification. Point 2, Figure 4

Table 4: Elemental Composition Taken from Spectrum 2 of Figure 4-Non-Activated Biochar at 8000X Magnification

Element	Weight%	Atomic%
C	94.35	97.18
O	3.08	2.38
K	0.48	0.15
Zr	2.08	0.28
Totals	100	

The EDS spectra of the points 1 and 2 in Figure 4 can be seen in Figure 5 and 6, respectively, along with the elemental composition of the spectra, Tables 3 and 4, respectively. High density compounds are expected to be found in spectrum 1 (Figure 4) as indicated by the backscatter image seen in Figure 3B. This is confirmed by the presence of Fe in the EDS spectrum (Figure 5) and the elemental composition of the spectrum, for which Fe represents 13.71% of the atomic composition (Table 3).

3.3.3.2 KOH-Activated Biochar

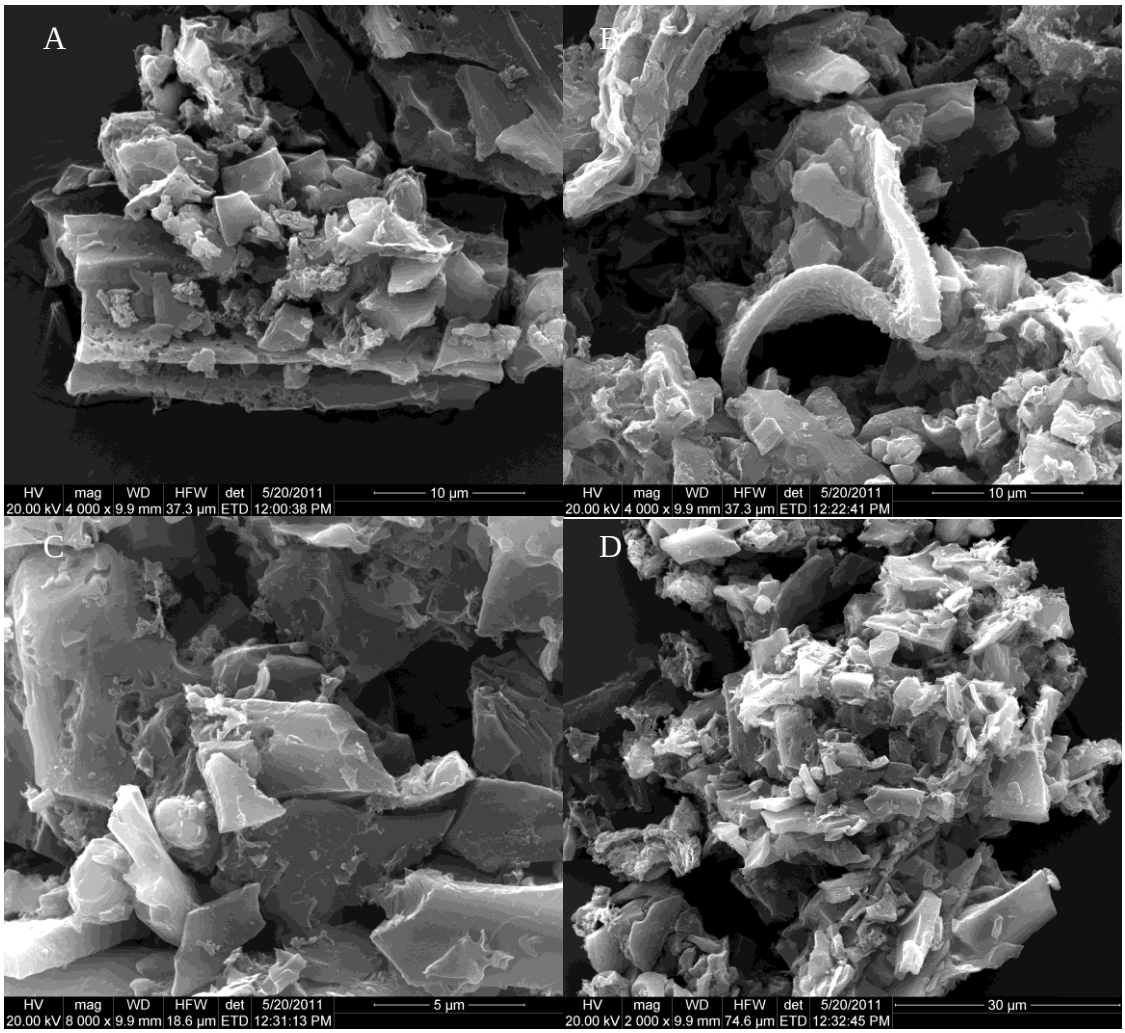

Figure 7: SEM Images of KOH-Activated Biochar at A) 4000X Magnification, B) 4000X, C) 8000X, and D) 2000X

The KOH-activated biochar under 4000X magnification (Figures 7A and 7B), 8000X (Figure 7C), and 2000X (Figure 7D) can be seen in Figure 7. The general structure is in contrast to the planar surfaces of the non-activated biochar seen in Figure 2. Likewise, the surface area of the KOH-activated char appears to be greater as

compared to the non-activated char. This is confirmed by the BET analysis, represented by Figure 1.

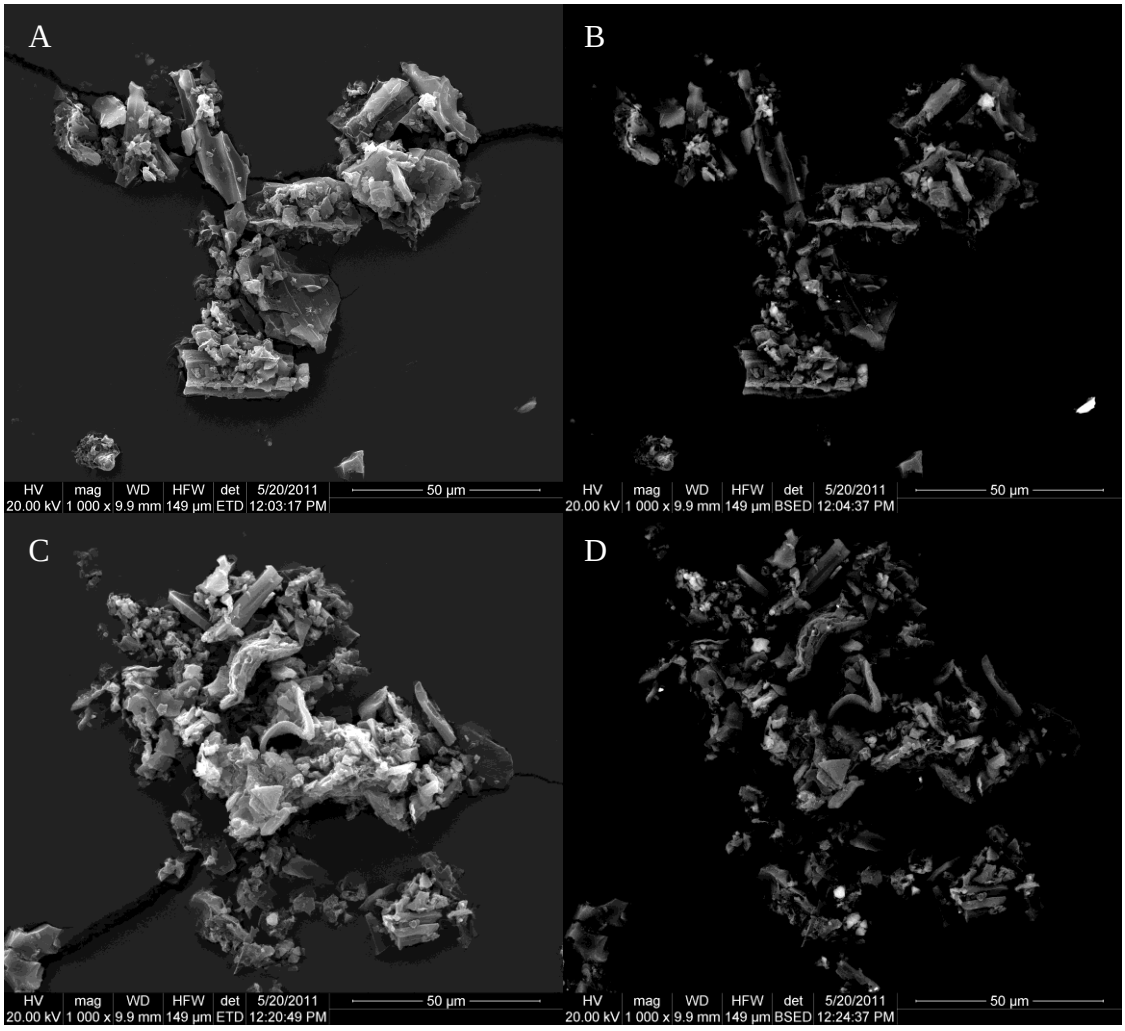

Figure 8: SEM Images of KOH-Activated Biochar at A) 1000X Magnification, B) Backscatter View of Image A, C) 1000X, and D) Backscatter View of Image C

Figure 8 represents the KOH-activated biochar at 1000X (Figures 8A and 8C) magnification with corresponding backscatter images (Figures 8B and 8D, respectively). As seen in Figure 8, the KOH-activation resulted in the presence of several particles of varying density.

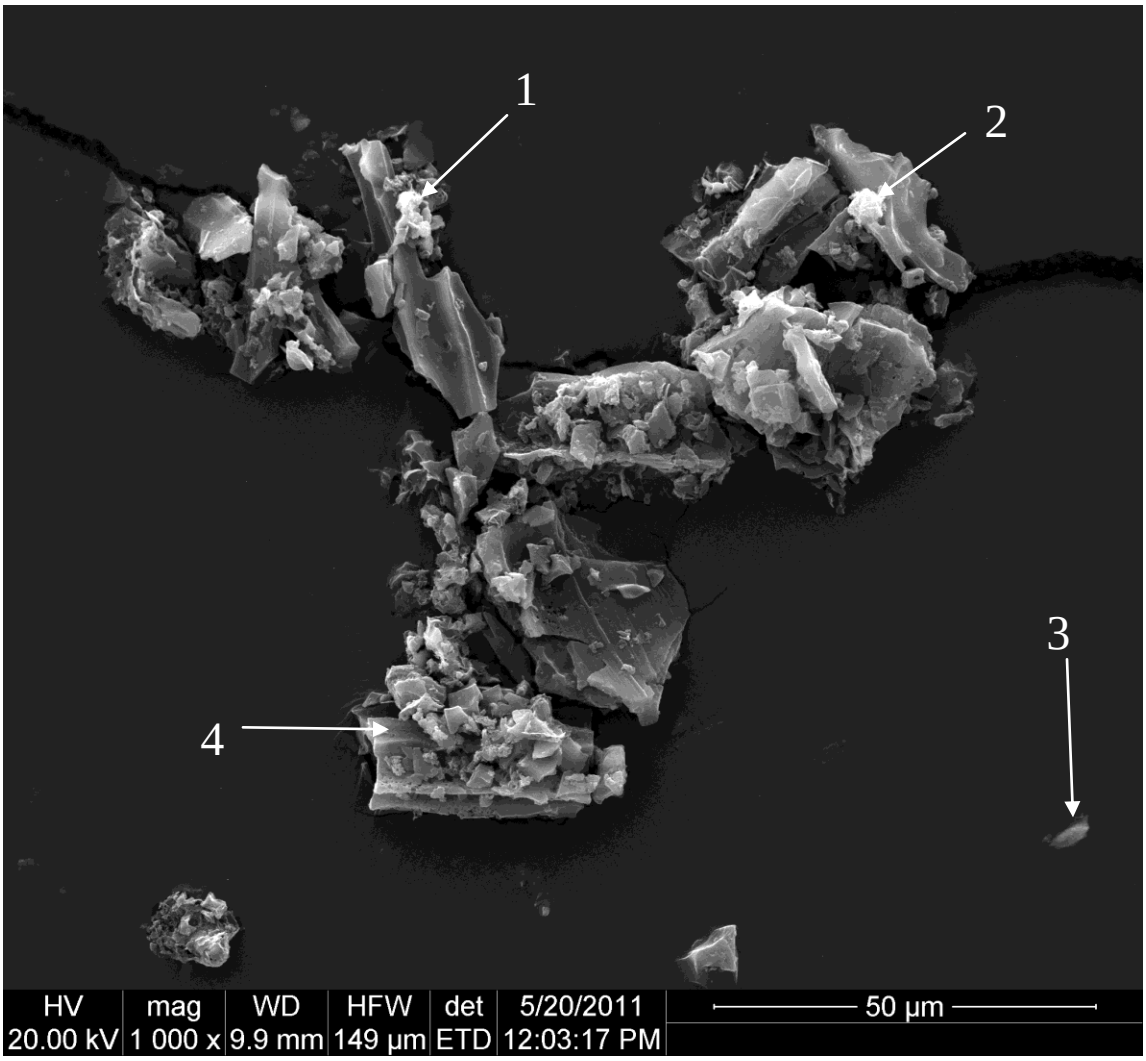

Figure 9: SEM Image of KOH-Activated Biochar at 1000X Magnification (from Figure 8A)

Figure 9 displays the selected points from which EDS spectra were captured. The resulting spectra and corresponding elemental composition tables can be seen below:

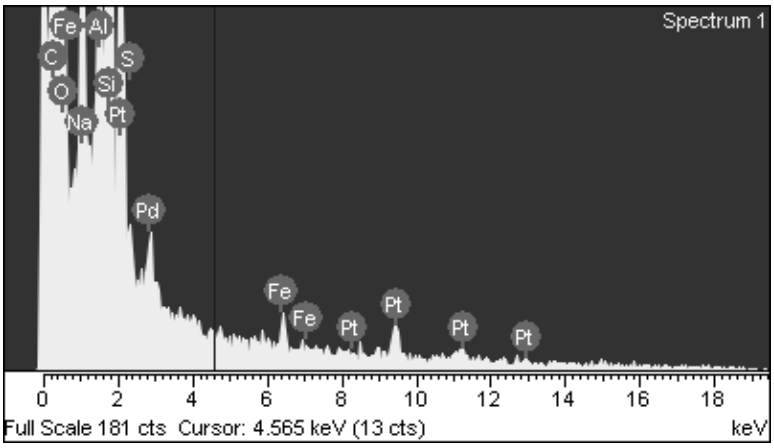

Figure 10: EDS Spectrum of KOH-Activated Biochar at 1000X Magnification. Point 1, Figure 9

Table 5: Elemental Composition Taken from Spectrum 1 of Figure 9-KOH-Activated Biochar at 1000X Magnification

Element	Weight%	Atomic%
C	27.44	43.46
O	26.56	31.58
Na	2.55	2.11
Al	3.01	2.12
Si	27.68	18.75
S	0.69	0.41
Fe	0.78	0.27
Pd	2.56	0.46
Pt	8.72	0.85
Totals	100	

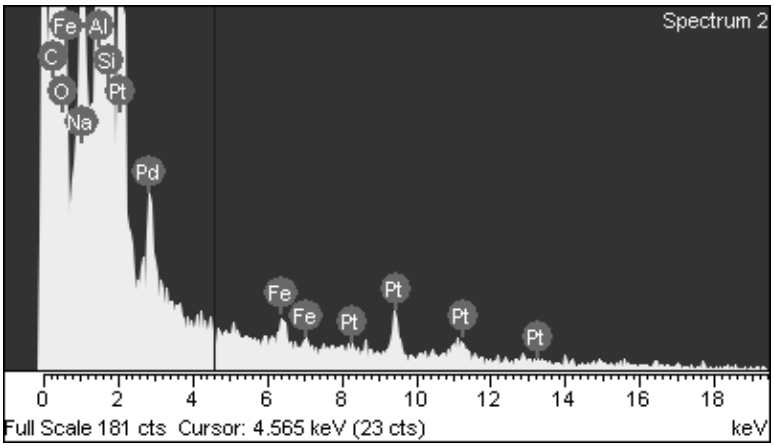

Figure 11: EDS Spectrum of KOH-Activated Biochar at 1000X Magnification. Point 2, Figure 9

Table 6: Elemental Composition Taken from Spectrum 2 of Figure 9-KOH-Activated Biochar at 1000X Magnification

Element	Weight%	Atomic%
C	12.92	23.61
O	28.32	38.86
Na	1.68	1.61
Al	4.02	3.27
Si	39.09	30.56
Fe	0.69	0.27
Pd	3.52	0.73
Pt	9.75	1.1
Totals	100	

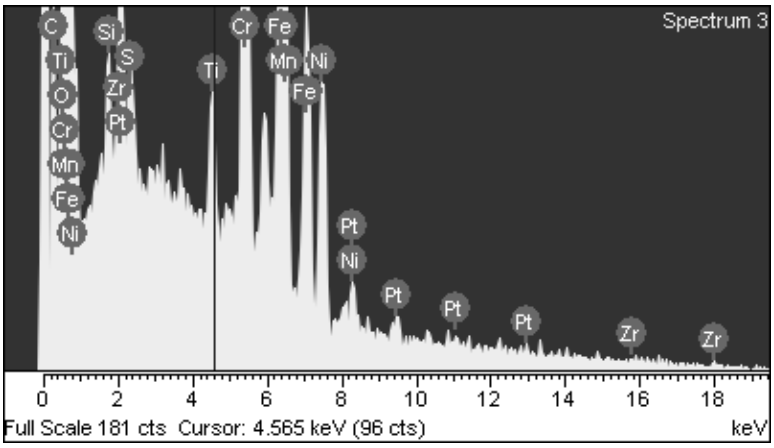

Figure 12: EDS Spectrum of KOH-Activated Biochar at 1000X Magnification. Point 3, Figure 9

Table 7: Elemental Composition Taken from Spectrum 3 of Figure 9-KOH-Activated Biochar at 1000X Magnification

Element	Weight%	Atomic%
C	2.27	9.31
O	2.02	6.2
Si	0.75	1.32
S	0.8	1.23
Ti	2.16	2.22
Cr	17.87	16.92
Mn	0.87	0.78
Fe	60.84	53.61
Ni	8.38	7.02
Zr	1.32	0.71
Pt	2.72	0.69
Totals	100	

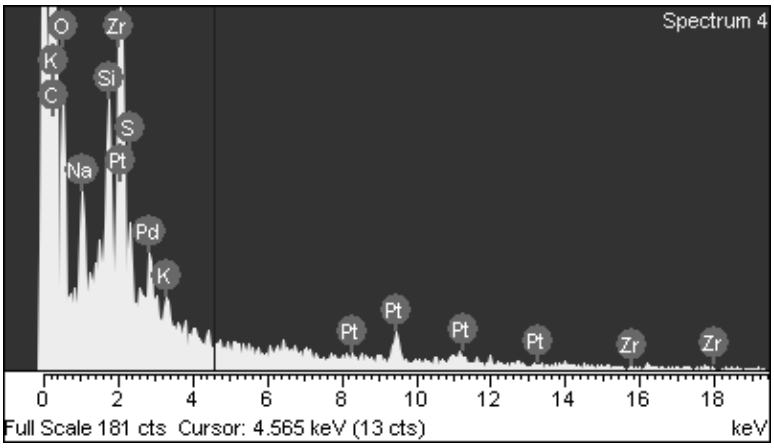

Figure 13: EDS Spectrum of KOH-Activated Biochar at 1000X Magnification. Point 4, Figure 9

Table 8: Elemental Composition Taken from Spectrum 4 of Figure 9-KOH-Activated Biochar at 1000X Magnification

Element	Weight%	Atomic%
C	69.92	89.76
O	3.93	3.78
Na	1.74	1.17
Si	3.25	1.78
S	1.6	0.77
K	0.78	0.31
Zr	7.45	1.26
Pd	4.15	0.6
Pt	7.18	0.57
Totals	100	

The EDS spectra of the points 1-4 in Figure 9 can be seen in Figures 10-13, along with the elemental composition of the spectra, Tables 5-8, respectively. As expected, based on the backscatter image, the particle representing point 3, Figure 9, contains high density elements, in this case Fe (53.6%, Table 7).

3.3.3.3 $ZnCl_2$-Activated Biochar

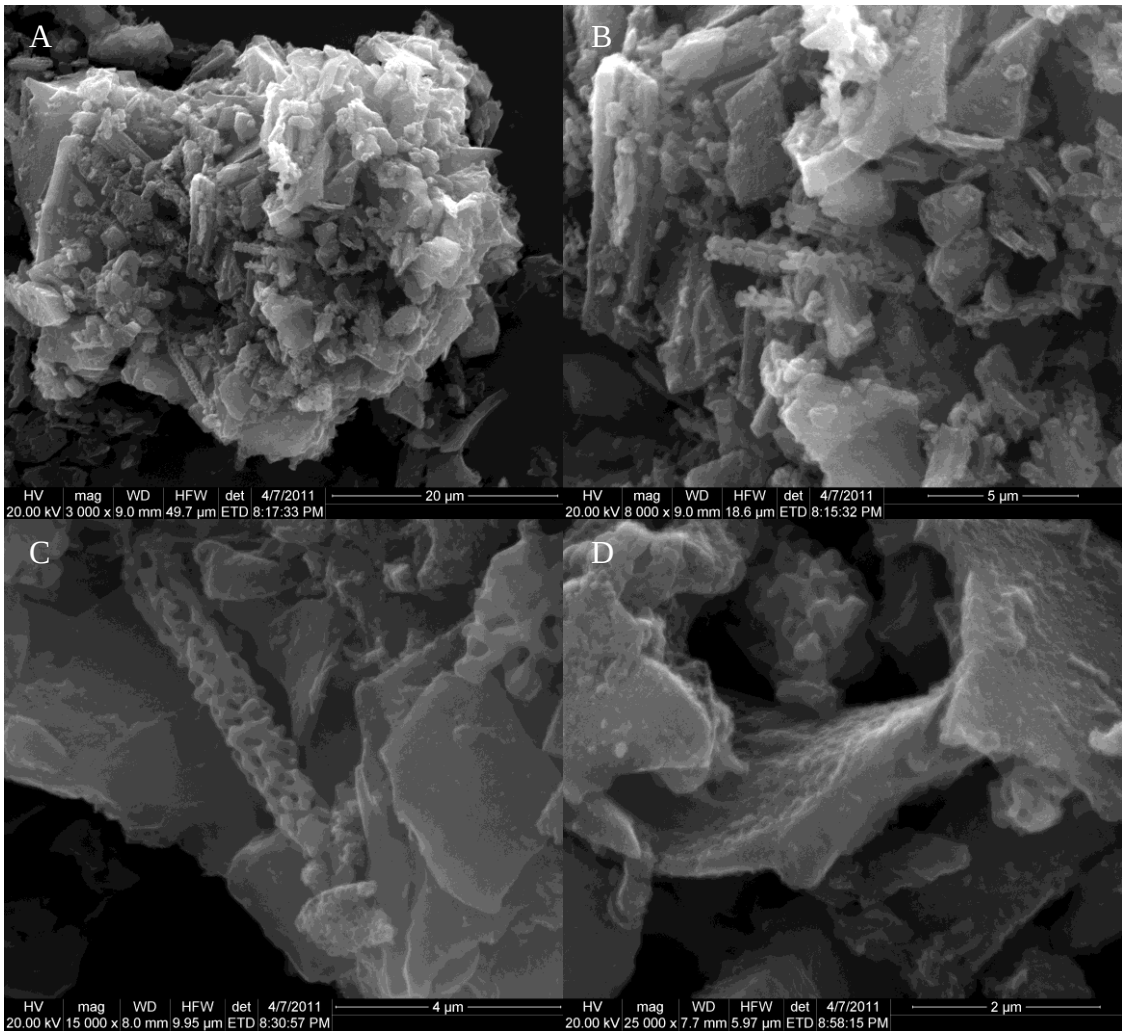

Figure 14: SEM Images of $ZnCl_2$-Activated Biochar at A) 3000X Magnification, B) 8000X, C) 15000X, and D) 25000X

The $ZnCl_2$-activated biochar can be seen at 3000X magnification, 8000X, 15000X, and 25000X (Figure 14A-14D, respectively). Porous structures and high surface area potential are evident in Figure 14. When viewing the material at 25000X, the texture of the activated surfaces can easily be seen.

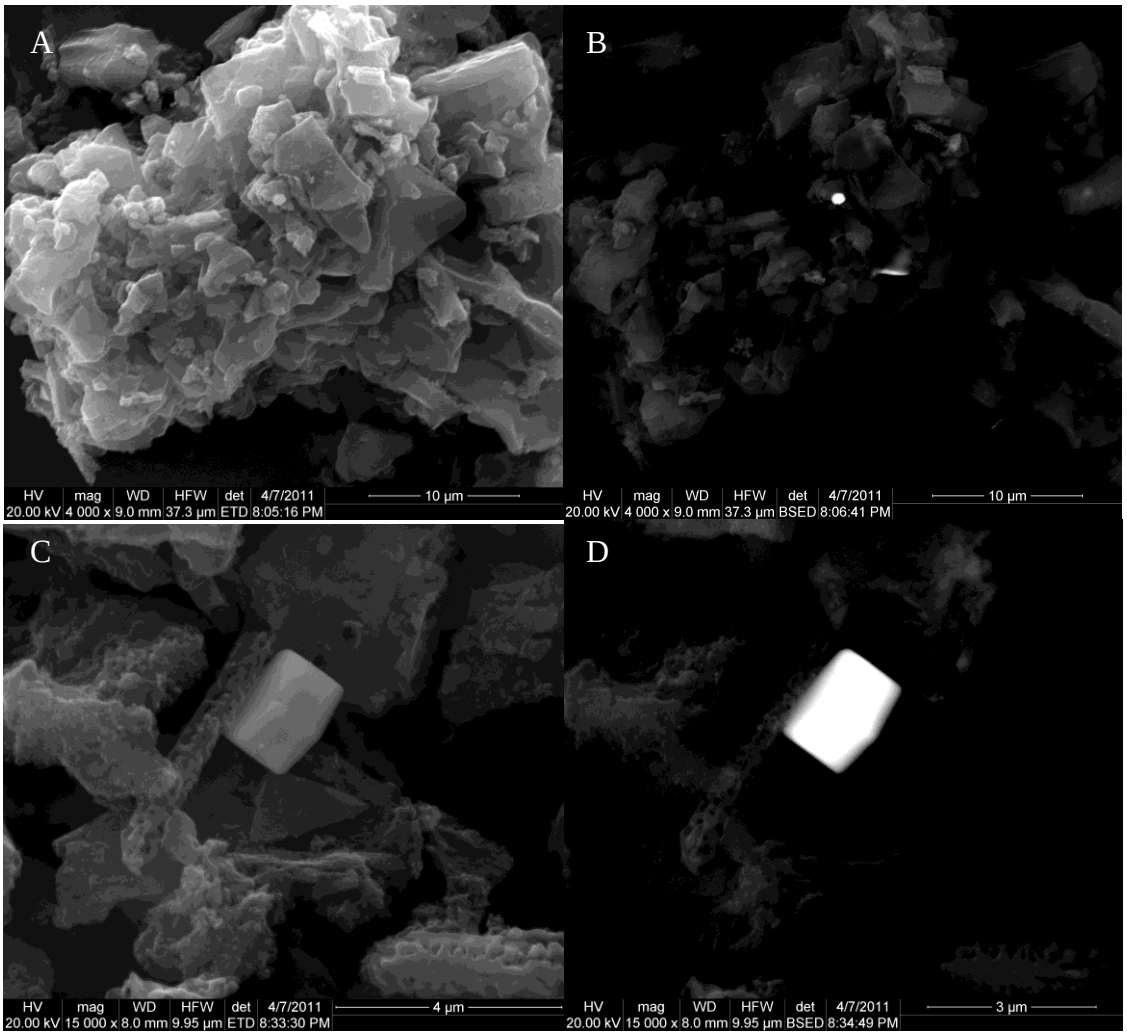

Figure 15: SEM Images of $ZnCl_2$-Activated Biochar at A) 4000X Magnification, B) Backscatter of Image A, C) 15000X, and D) Backscatter of Image C

High density particles in the $ZnCl_2$-activated biochar can be seen in Figure 15 at 4000 and 16000X magnification (B and D, respectively).

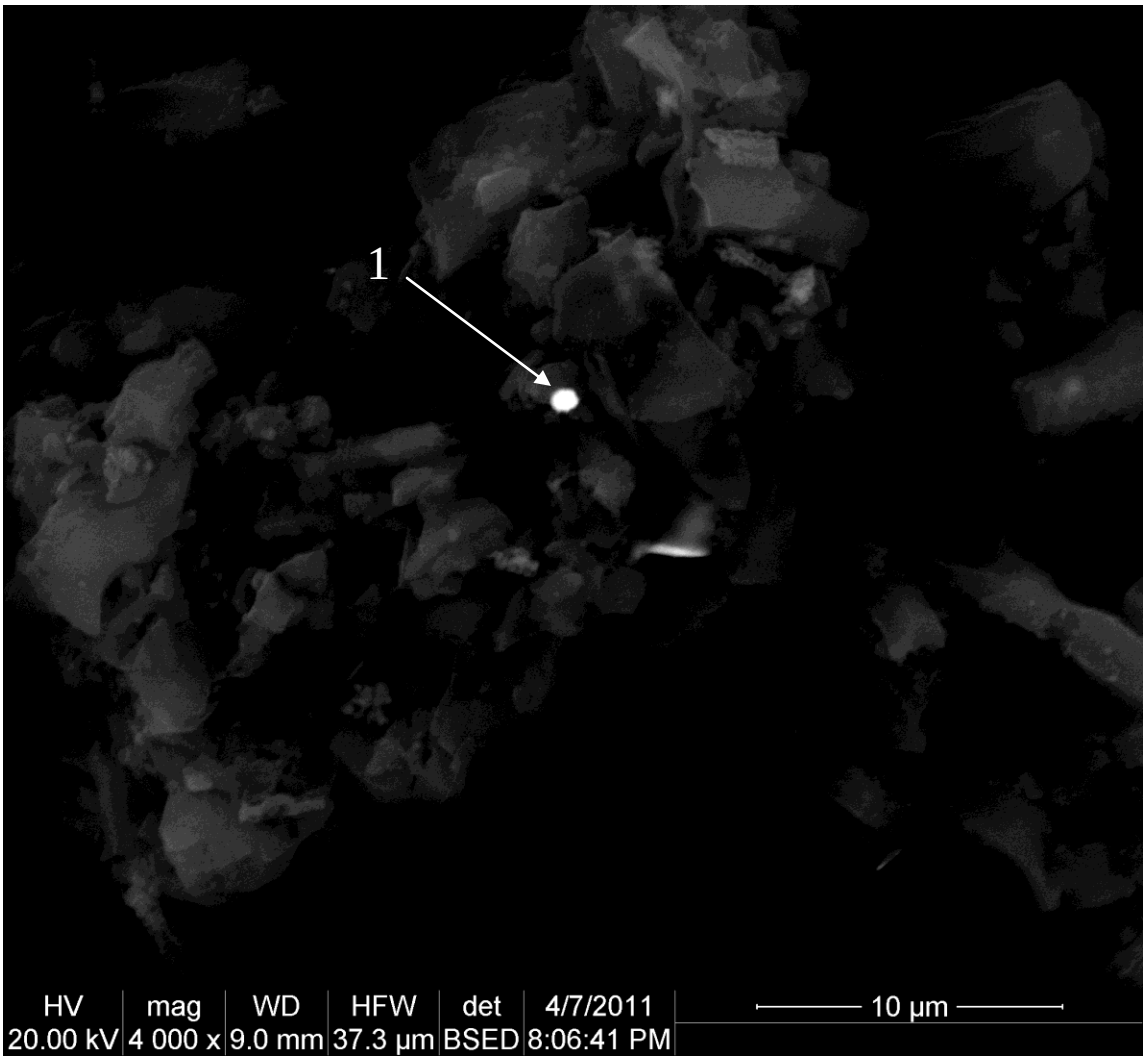

Figure 16: SEM Backscatter Image of $ZnCl_2$-Activated Biochar at 4000X Magnification (from Figure 15B)

Elemental composition and an EDS spectrum were taken from point 1, seen in Figure 16. The resulting spectrum and elemental table can be seen in Figure 17 and Table 9.

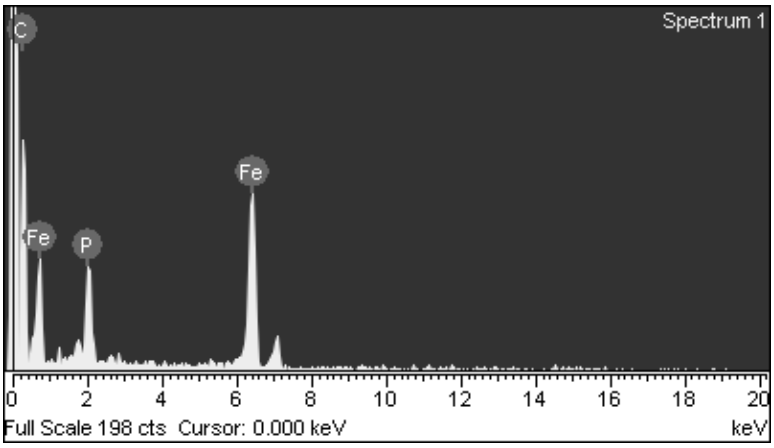

Figure 17: EDS Spectrum of $ZnCl_2$-Activated Biochar at 4000X Magnification. Point 1, Figure 16

Table 9: Elemental Composition Taken from Spectrum 1 of Figure 16-$ZnCl_2$-Activated Biochar at 4000X Magnification

Element	Weight%	Atomic%
C	28.71	62.62
P	10.47	8.85
Fe	60.82	28.53
Totals	100	

The evidence presented by the backscatter image (Figure 16), EDS spectrum (Figure 17), and the elemental composition (Table 9) of the high density particle in the above image suggests the presence/formation of iron-phosphates in the $ZnCl_2$-activated samples.

3.3.3.4 H_3PO_4-Activated Biochar

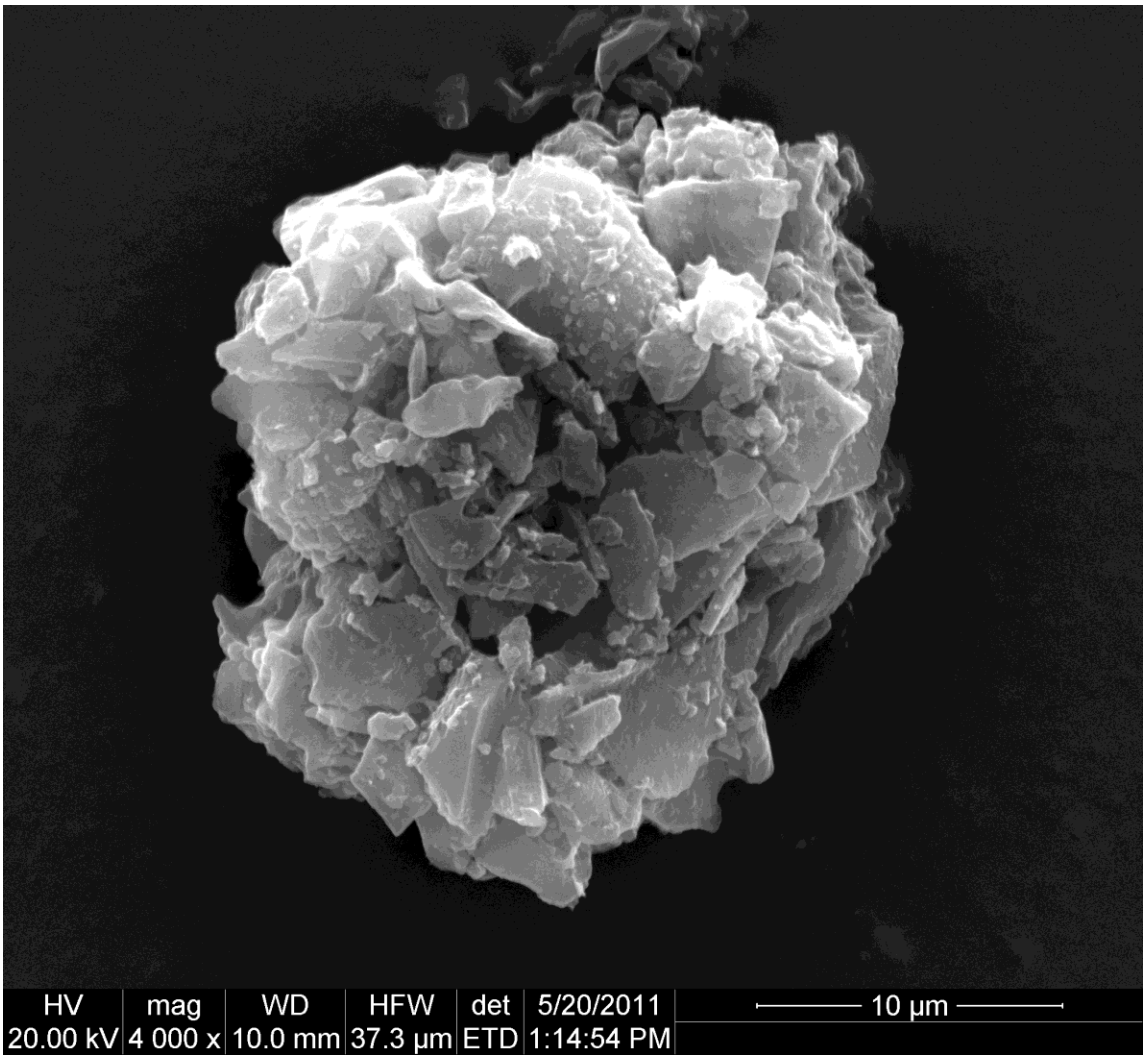

Figure 18: SEM Image of H_3PO_4-Activated Biochar at 4000X Magnification

Figure 18 displays H_3PO_4-activated biochar at 4000X magnification. As can be seen in Figure 18, the result of the activation process was a product that would appear to have greater surface area potential when compared to the non-activated char. The surfaces appear to have more texture and the sample would appear to have more overall surface area.

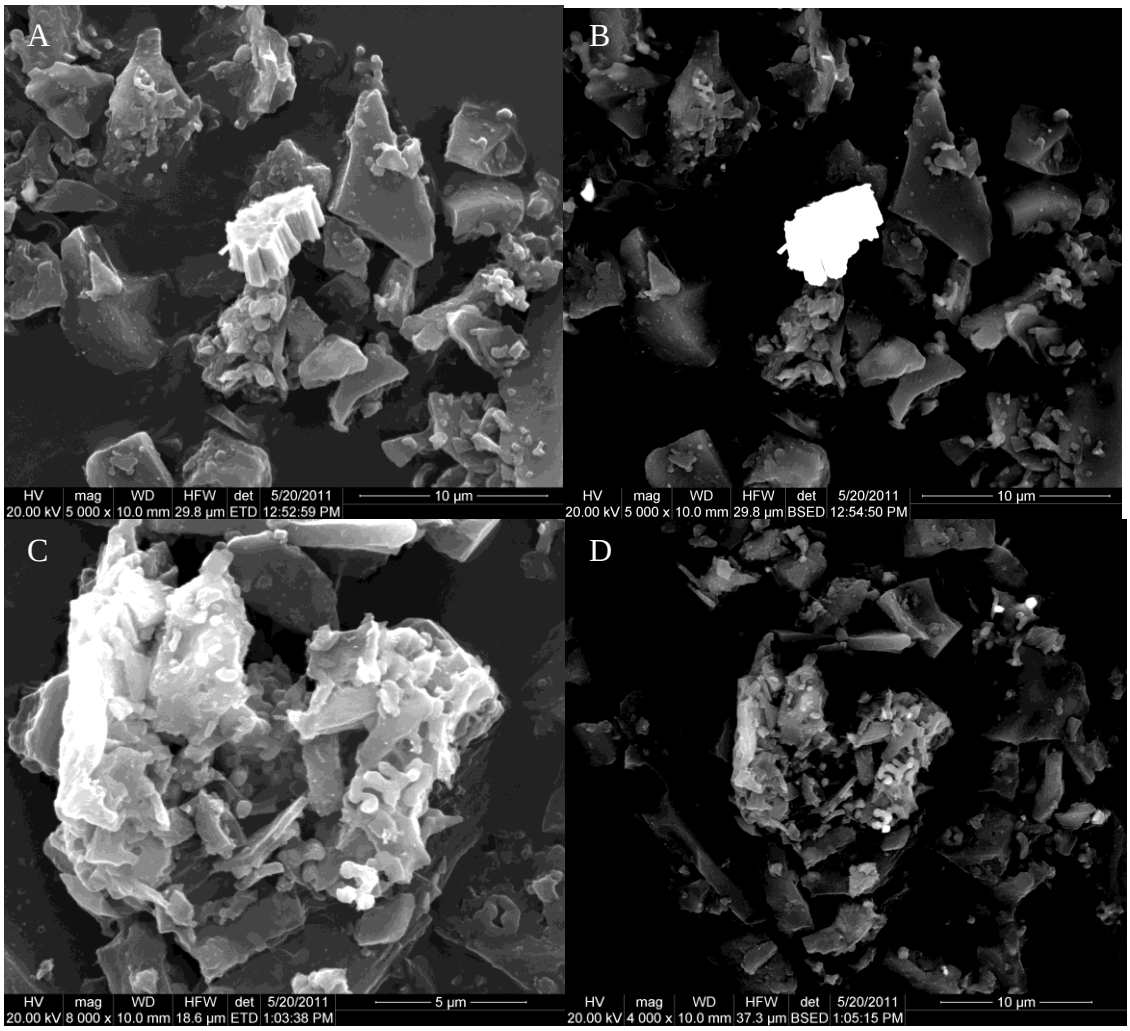

Figure 19: SEM Images of H_3PO_4-Activated Biochar at A) 5000X Magnification, B) Backscatter View of Image A, C) 8000X, and D) 4000X Backscatter View of Image C

As seen in Figure 19, the H_3PO_4-activated biochar contains a number of high density fragments. This is apparent when viewing the backscatter images (Figure 19B and 19D) above. A closer look at the image (Figure 20) indicates that not only are particles of very high density present, but that most of the material comprising the H_3PO_4-activated biochar is also generally dense material, as compared to the other

treatments. This is indicated by the relative ease at which the material is viewed in the backscatter image.

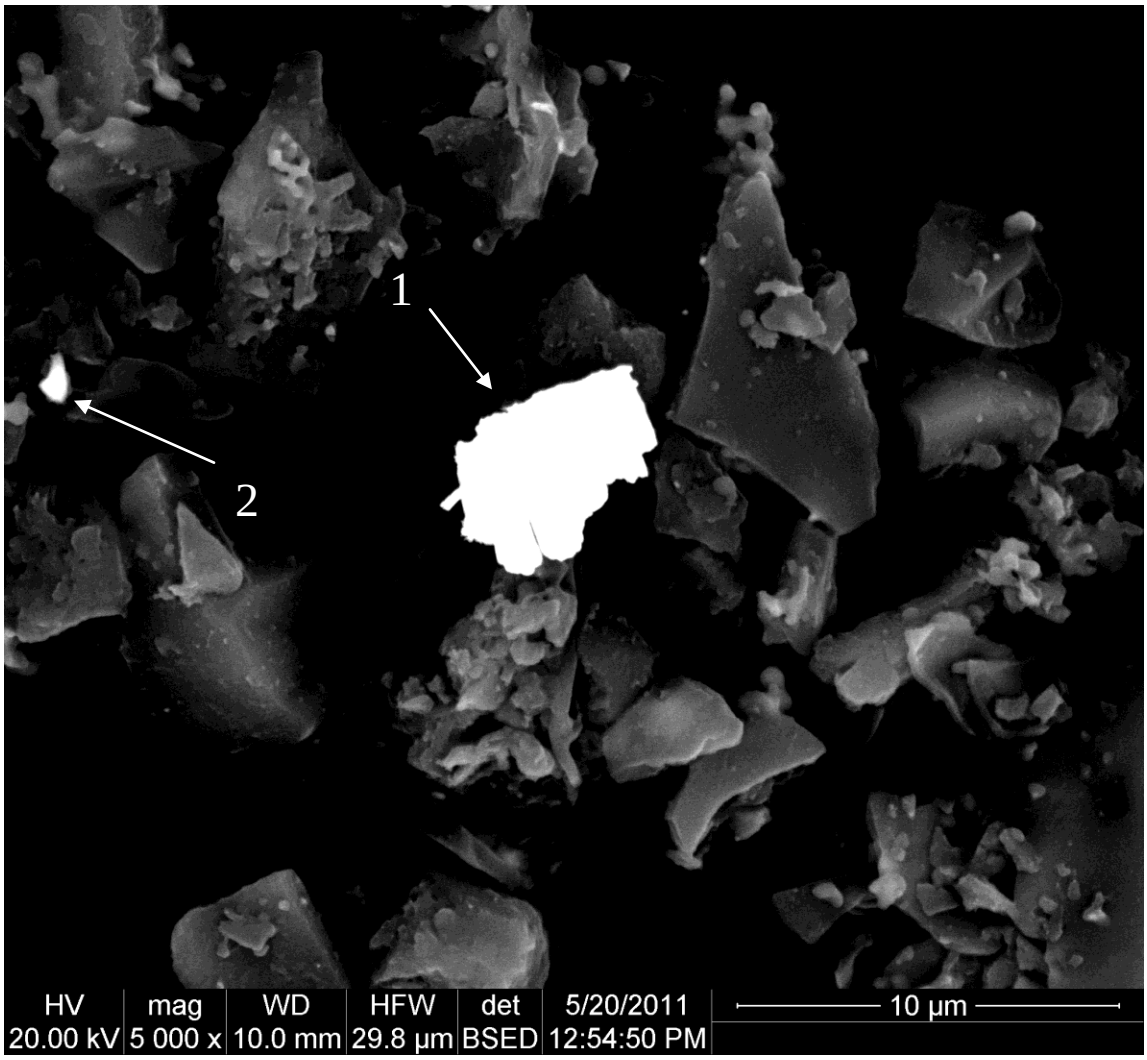

Figure 20: SEM Backscatter Image of H_3PO_4-Activated Biochar at 5000X Magnification (from Figure 19B)

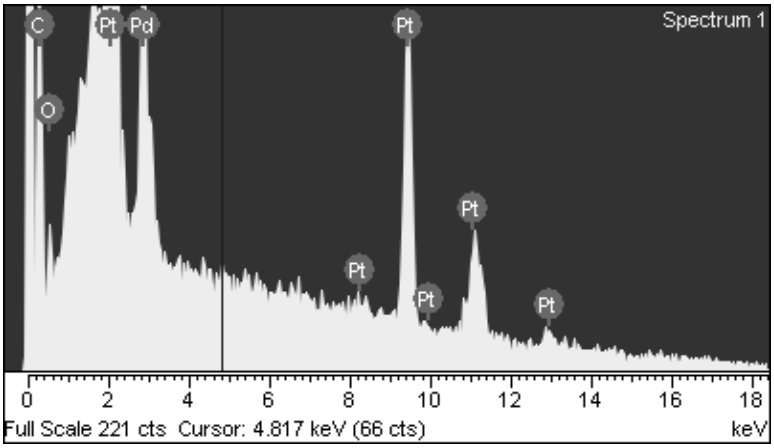

Figure 21: EDS Spectrum of H_3PO_4-Activated Biochar at 5000X Magnification. Point 1, Figure 20

Table 10: Elemental Composition Taken from Spectrum 1 of Figure 20-H_3PO_4-Activated Biochar at 5000X Magnification

Element	Weight%	Atomic%
C	3.44	32.39
O	0.75	5.31
Pd	14.19	15.06
Pt	81.61	47.24
Totals	100	

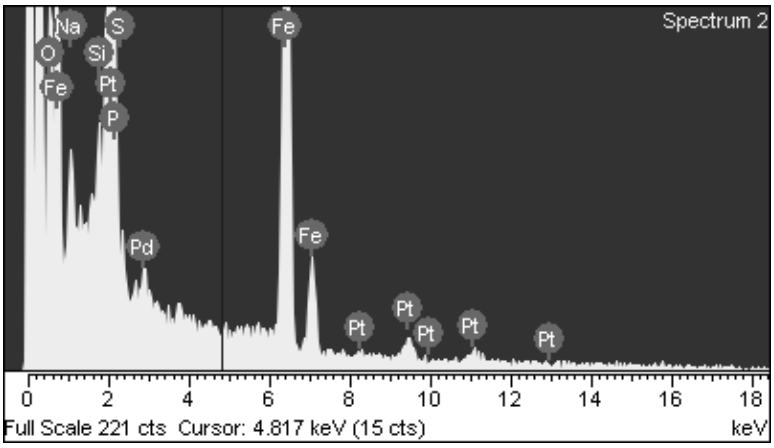

Figure 22: EDS Spectrum of H_3PO_4-Activated Biochar at 5000X Magnification. Point 2, Figure 20

Table 11: Elemental Composition Taken from Spectrum 2 of Figure 20-H_3PO_4-Activated Biochar at 5000X Magnification

Element	Weight%	Atomic%
O	3.21	8.61
Na	1.43	2.68
Si	1.51	2.31
P	33.12	45.91
S	0.92	1.23
Fe	46.59	35.81
Pd	3	1.21
Pt	10.21	2.25
Totals	100	

Significant spikes in both platinum and palladium can be seen in the EDS spectrum of point 1 (Figure 21). This may be the result of the SEM coating for which a 4.0 nm thick platinum/palladium alloy was used in sample preparation. As indicated by Table 10, the total, combined, atomic percentage of platinum and palladium in the particle was 62.3%. While this particle may have been associated with SEM preparation rather than the H_3PO_4 activation process, the same cannot be said for the particle at point 2 (Figure 20). Here, as seen in the $ZnCl_2$-activated biochar, can be found evidence of iron phosphate presence/formation. The EDS spectrum for point 2 shows distinct spikes indicative of Fe and P (Figure 22). This is confirmed by the elemental analysis (Table 11) in which Fe and P constitute 35.81% and 45.91%, respectively, of the atomic percentage.

3.3.3.5 Darco® S-51 PAC

Darco® S-51 PAC was also viewed with the SEM for comparison with treatment PACs. The results of which can be seen in Figure 23. As seen in the above image, Darco® S-51 contains a number of irregularly shaped particles with fair surface texture. Taken together, the potential surface area appears to be greater than that of the non-activated biochar but not as substantial as the treatment PACs. This observation is confirmed by the BET surface area analysis (Figure 1).

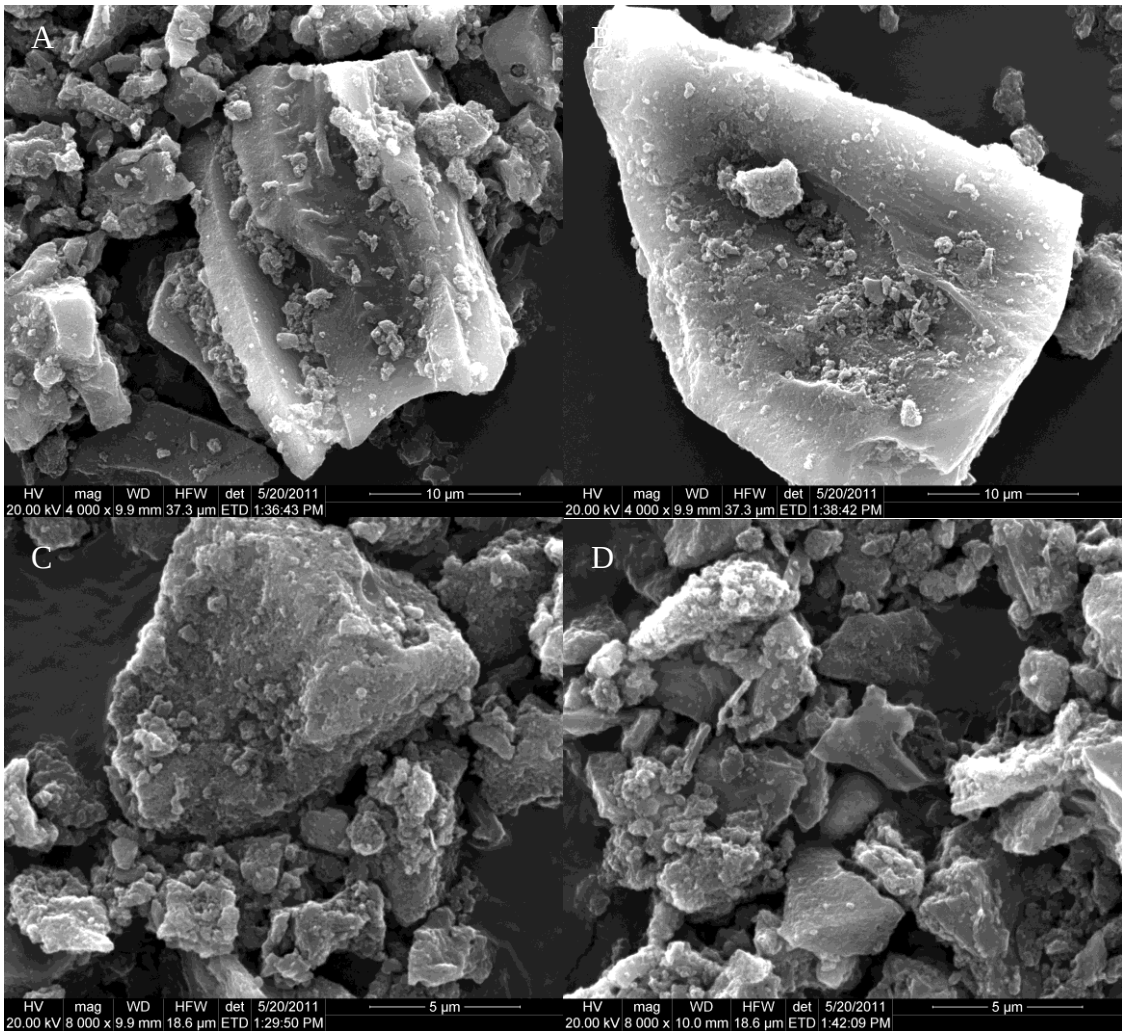

Figure 23: SEM Images of Darco® S-51 PAC at 4000X Magnification (A and B) and 8000X (D and C)

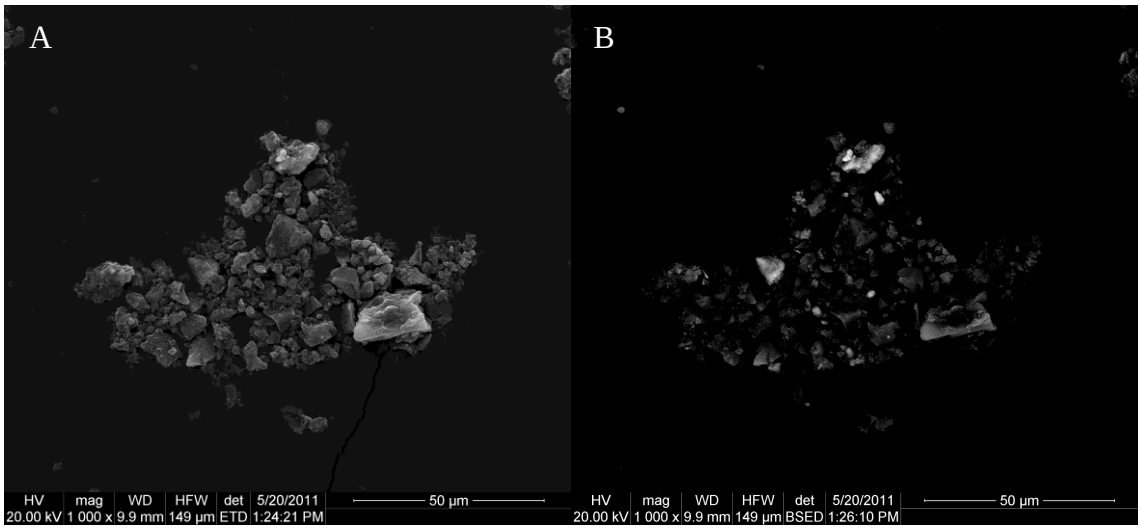

Figure 24: SEM Images of Darco® S-51 at A) 1000X Magnification and B) Backscatter View of Image A

As can be seen in Figure 24, the Darco® S-51 PAC also contains particles of high density. This is particularly distinguishable in the bright particles of the backscatter image (Figure 24B).

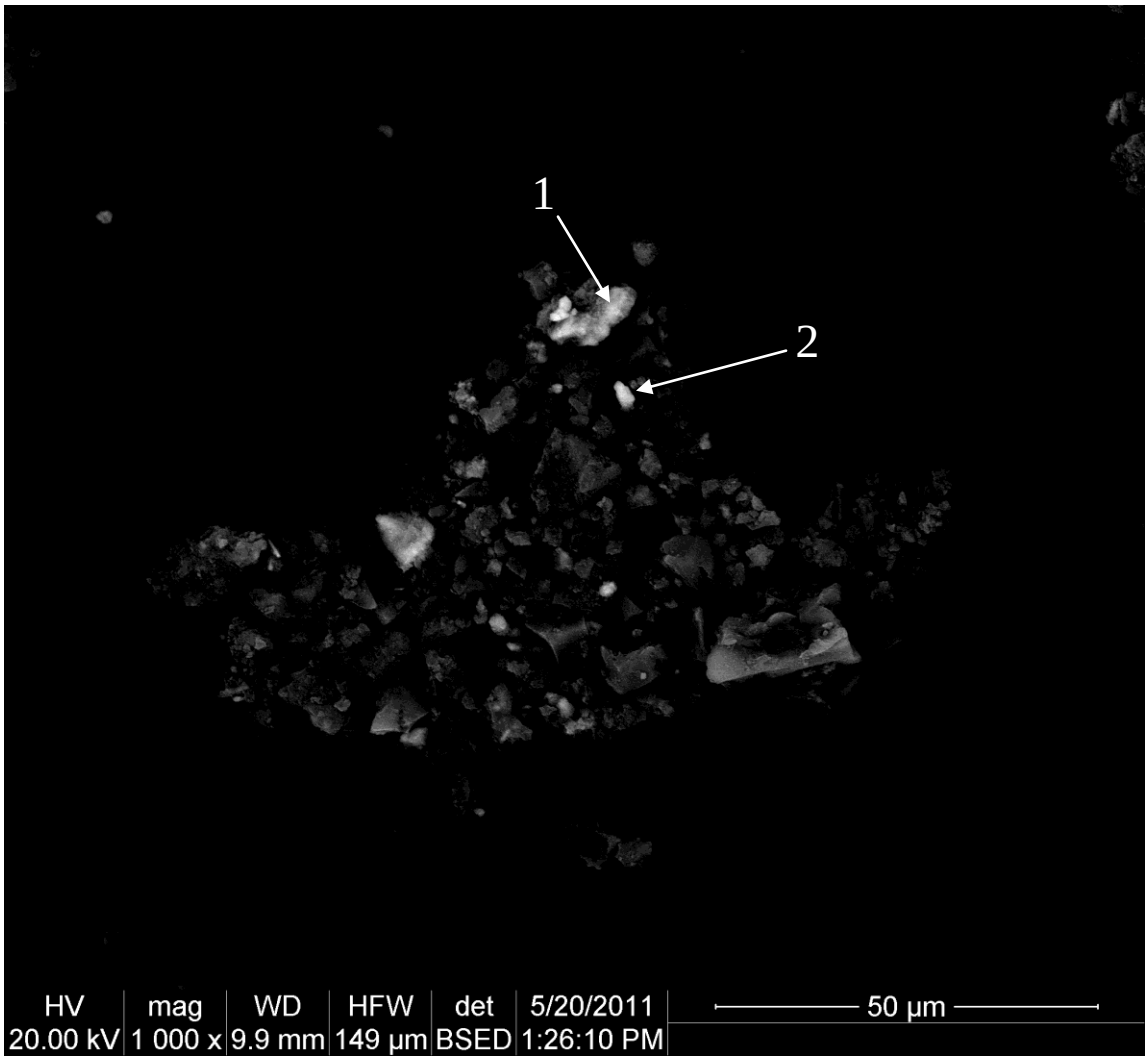

Figure 25: SEM Backscatter Image of Darco® S-51 PAC at 1000X Magnification (from Figure 24B)

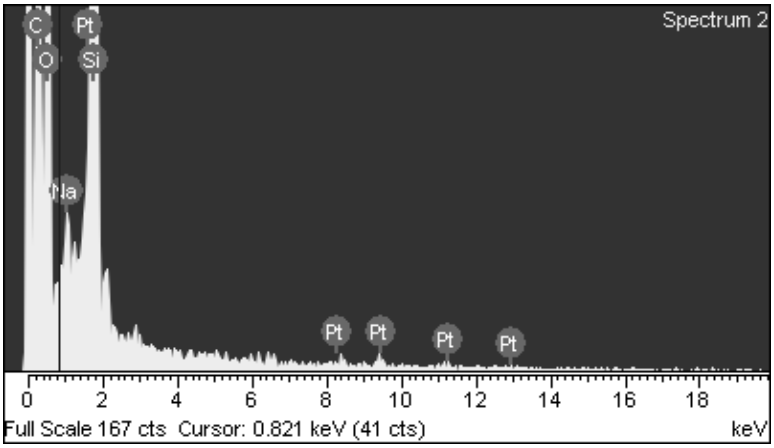

Figure 26: EDS Spectrum of Darco® S-51 PAC at 1000X Magnification. Point 1, Figure 25

Table 12: Elemental Composition Taken from Spectrum 1 of Figure 25-Darco® S-51 PAC at 1000X Magnification

Element	Weight%	Atomic%
O	24.74	38.25
Na	1.22	1.31
Al	4.29	3.94
Si	61.06	53.78
K	1.00	0.63
Zr	7.69	2.09
Totals	100	

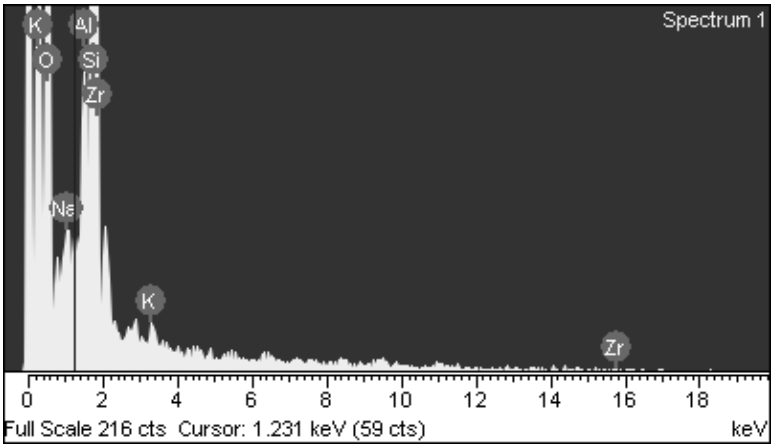

Figure 27: EDS Spectrum of Darco® S-51 PAC at 1000X Magnification. Point 2, Figure 25

Table 13: Elemental Composition Taken from Spectrum 2 of Figure 25-Darco® S-51 PAC at 1000X Magnification

Element	Weight%	Atomic%
C	24.31	38.83
O	21.71	26.04
Na	1.43	1.19
Si	49.20	33.61
Pt	3.35	0.33
Totals	100	

As indicated by the EDS spectra (Figures 26 and 27) and elemental composition (Tables 12 and 13), the particles of higher density, present in the Darco® S-51 PAC, are not of metal origin, unlike most of the high density particles found in the activated biochars. Rather, the dense particles present in the Darco® S-51 seem to be related to the presence of siliceous compounds. Because oxygen is also present in proportionally greater quantities, these particles are likely silicon oxide.

3.4 Surface and Groundwater Characterization

3.4.1 pH, Conductivity, and N, P, C

The results of the environmental water pH, conductivity, N, P, and C, can be seen in Table 14. All values, with exception of pH and conductivity, are expressed in mg/L. As expected, almost all values are greater in the surface water, as compared to the groundwater.

3.4.2 Anions, Cations, and Surface Water *E. coli* Concentration

The results of the anion and cation concentration analysis can be seen in Table 15; all values are expressed in mg/L. Again, the surface water concentrations are, in all instances, greater than that of the groundwater. The increase in concentrations of Na^+ and Cl^- in surface water samples, as compared to groundwater, is in agreement with conductivity differences between the two water samples. The surface water *E. coli* concentration was determined to be 300 colony forming units (CFU) per 100 m

Table 14: Selected Characteristics of Surface and Groundwater Samples Used in This Study

	Parameter							
	pH	Conductivity	NO_3-N	NH_3-N	PO_4-P	NPOC	TN	DON
Sample ID		µS/cm	----------mg/l ----------					
Surface Water Mean	8.58 ± 0.05	1830 ± 26.5	0.324 ± 0.01	0.1405 ± 0.01	0.830 ± 0.02	14.572 ± 0.5	1.166 ± 0.01	0.701 ± 0.03
Groundwater Mean	8.67 ± 0.09	923 ± 49.3	0.102 ± 0.003	0.487 ± 0.05	N/A	3.395 ± 1.2	0.627 ± 0.03	0.038 ± 0.04

WPC: Wolf Pen Creek, ND: None Detected, N/A: Not Applicable

Table 15: Selected Anions and Cations of Surface and Groundwater Samples Used in This study

	Parameter							
	F^-	Cl^-	NO_3^-	SO_4^{2-}	Na^+	K^+	Mg^{2+}	Ca^{2+}
Sample ID	----------mg/l ----------							
Surface Water Mean	0.9663 ± 0.1	145.922 ± 8.6	1.4253 ± 0.05	69.670 ± 3.1	394.902 ± 4.8	5.814 ± 0.3	2.693 ± 0.1	17.280 ± 0.9
Groundwater Mean	0.3754 ± 0.2	47.688 ± 0.8	0.4489 ± 0.01	18.690 ± 3.0	207.392 ± 0.9	2.607 ± 0.07	0.7230 ± 0.1	3.300 ± 1.1

WPC: Wolf Pen Creek, ND: None Detected, N/A: Not Applicable

3.5 Batch Analyses

3.5.1 Effects of Non-Activated Biochar on MS2 Levels

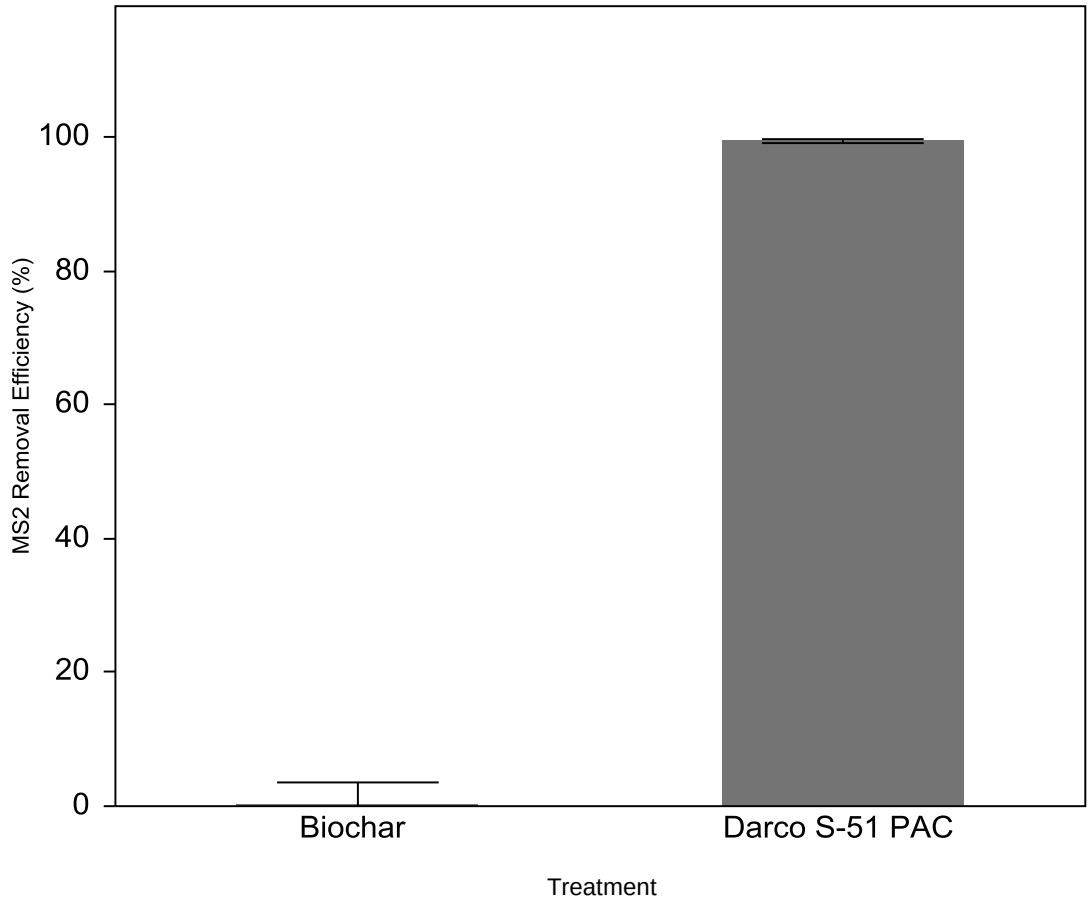

Figure 28: Effects of Non-Activated Char on MS2 in PBS. Error Bars Represent Standard Error of Six Replications

Non-activated biochar appeared to have little to no effect on MS2 levels in PBS (Figure 28). Darco® S-51, however, appeared to be very efficient (99.5%) in MS2 removal, as seen in Figure 28. As mentioned, removal efficiency was based on plate count numbers (PFU/mL) of batch filtrates.

Table 16: Means and Standard Deviations for Non-Activated Biochar Effects on MS2 Levels (PFU/mL) in PBS

Batch	N	Mean	Std Dev	Std Err Mean	Lower 95%	Upper 95%
Biochar	20	60.60	14.00	3.13	54.05	67.15
Darco S-51 PAC	18	0.28	0.58	0.14	-0.01	0.56
Baseline	20	60.80	13.82	3.09	54.33	67.27

Means and standard deviations of filtrate plate counts can be seen in Table 16. The mean PFU/mL within the non-activated biochar batch and the baseline batch were separated by only 0.2 PFU/mL. These two batches could not be statistically delineated using the student's t-test with a type 1 error (α) of 0.05 (Table 17).

Table 17: Student's t-test for Non-Activated Biochar Effects on MS2 Levels (PFU/mL) (α: 0.05)

Level	- Level	Difference	Std Err Dif	Lower CL	Upper CL	p-Value
Baseline	Darco S-51	60.52	3.76	52.99	68.05	<.0001
Biochar	Darco S-51	60.32	3.76	52.79	67.85	<.0001
Baseline	Biochar	0.2	3.66	-7.13	7.53	0.957

3.5.2 Effects of Activated Biochars on MS2 Levels in PBS

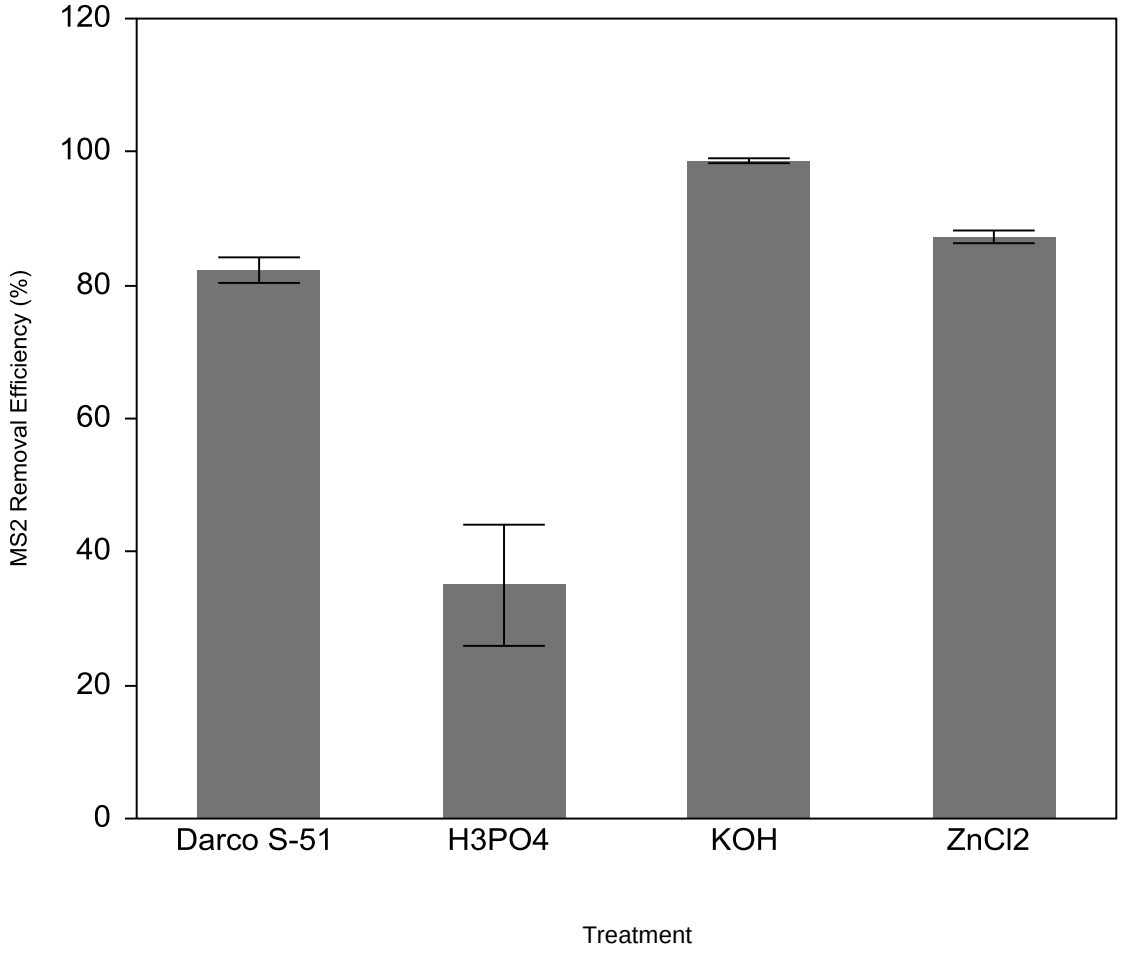

Figure 29: Effects of Activated Biochars on MS2 Levels in PBS. Error Bars Represent Standard Error of Four Replications

The activated biochars had a much more positive effect on MS2 removal, as compared to non-activated biochars. Baseline infectivity (seeding rate) ranged from 2.5 – 6.25 x 10^9 PFU/mL. At that rate, the KOH-activated biochar performed the best, removing a mean of 98.68% of MS2 particles (Table 18).

Table 18: Means and Standard Deviations for Activated Biochar Effects on MS2 Levels (PFU/mL) in PBS

Batch	N	Mean	Std Dev	Std Err Mean	Lower 95%	Upper 95%
Darco S-51	4	82.27	3.84	1.92	76.16	88.37
H_3PO_4	4	35.00	18.18	9.09	6.07	63.92
KOH	4	98.68	0.74	0.37	97.51	99.85
$ZnCl_2$	4	87.26	1.90	0.95	84.23	90.29

Statistical delineation of treatment effects was possible for most batches at an α: 0.05 (Table 19), as evidenced by the student's t-test.

Table 19: Student's t-test for Activated Biochar Effects on MS2 Levels (PFU/mL) in PBS (α: 0.05)

Level	- Level	Difference	Std Err Dif	Lower CL	Upper CL	p-Value
KOH	H_3PO_4	63.68	6.61	49.29	78.08	<.0001
$ZnCl_2$	H_3PO_4	52.27	6.61	37.87	66.66	<.0001
Darco S-51	H_3PO_4	47.27	6.61	32.88	61.67	<.0001
KOH	Darco S-51	16.41	6.61	2.01	30.81	0.0288
KOH	$ZnCl_2$	11.42	6.61	-2.98	25.81	0.1096
$ZnCl_2$	Darco S-51	4.99	6.61	-9.40	19.39	0.4644

Significant differences were found in all treatments except those between the KOH and $ZnCl_2$ treatments and the Darco® S-51 and $ZnCl_2$ treatment. The KOH treatment was most effective in MS2 removal followed by the $ZnCl_2$ treatment, both of which were more effective than Darco® S-51. The H_3PO_4 treatment, however, was the least effective in MS2 removal.

3.5.3 Effects of Activated Biochars on MS2 Levels in Surface Water

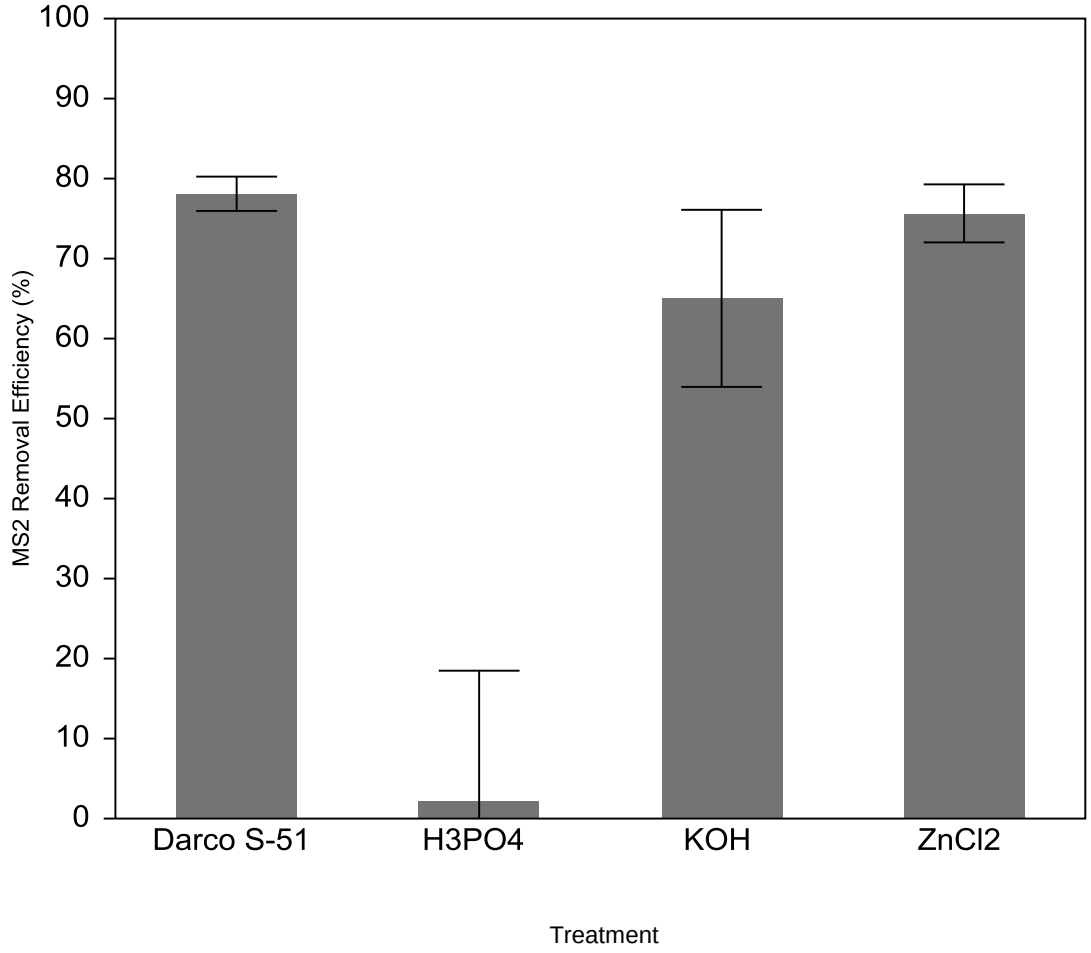

Figure 30: Effects of Activated Biochars on MS2 Levels in Surface Water. Error Bars Represent Standard Error of Three Replications

The surface water removal efficiency of MS2 by the activated biochars can be seen in Figure 30. The baseline infectivity/seeding rate was greatly, and necessarily, reduced for surface water batches. Infectivity of baseline batches ranged from 8,400 – 15,133 PFU/mL. At that rate, Darco® S-51performed most favorably, having a removal efficiency of 78.10% (Table 20). Though the Darco® S-51was numerically the most

effective, statistical delineation among treatments was not possible, with exception of the H_3PO_4-activated biochar (Table 21).

Table 20: Means and Standard Deviations for Activated Biochar Effects on MS2 Levels (PFU/mL) in Surface Water

Batch	N	Mean	Std Dev	Std Err Mean	Lower 95%	Upper 95%
Darco S-51	3	78.10	3.71	2.14	68.88	87.33
H_3PO_4	3	2.26	28.10	16.22	-67.54	72.07
KOH	3	65.03	19.17	11.07	17.40	112.66
$ZnCl_2$	3	75.65	6.28	3.63	60.05	91.25

The effects of the H_3PO_4-activated biochar were negligible, having a mean removal efficiency of only 2.26% and the greatest variability (Table 20).

Table 21: Student's t-test for Activated Biochar Effects on MS2 Levels (PFU/mL) in Surface Water (α: 0.05)

Level	- Level	Difference	Std Err Dif	Lower CL	Upper CL	p-Value
Darco S-51	H_3PO_4	75.84	14.20	43.08	108.59	0.0007
$ZnCl_2$	H_3PO_4	73.39	14.20	40.63	106.14	0.0009
KOH	H_3PO_4	62.76	14.20	30.01	95.52	0.0022
Darco S-51	KOH	13.07	14.20	-19.68	45.83	0.3842
$ZnCl_2$	KOH	10.62	14.20	-22.13	43.38	0.4759
Darco S-51	$ZnCl_2$	2.45	14.20	-30.30	35.20	0.8673

3.5.4 Effects of Activated Biochars on ΦX174 Levels in Surface Water

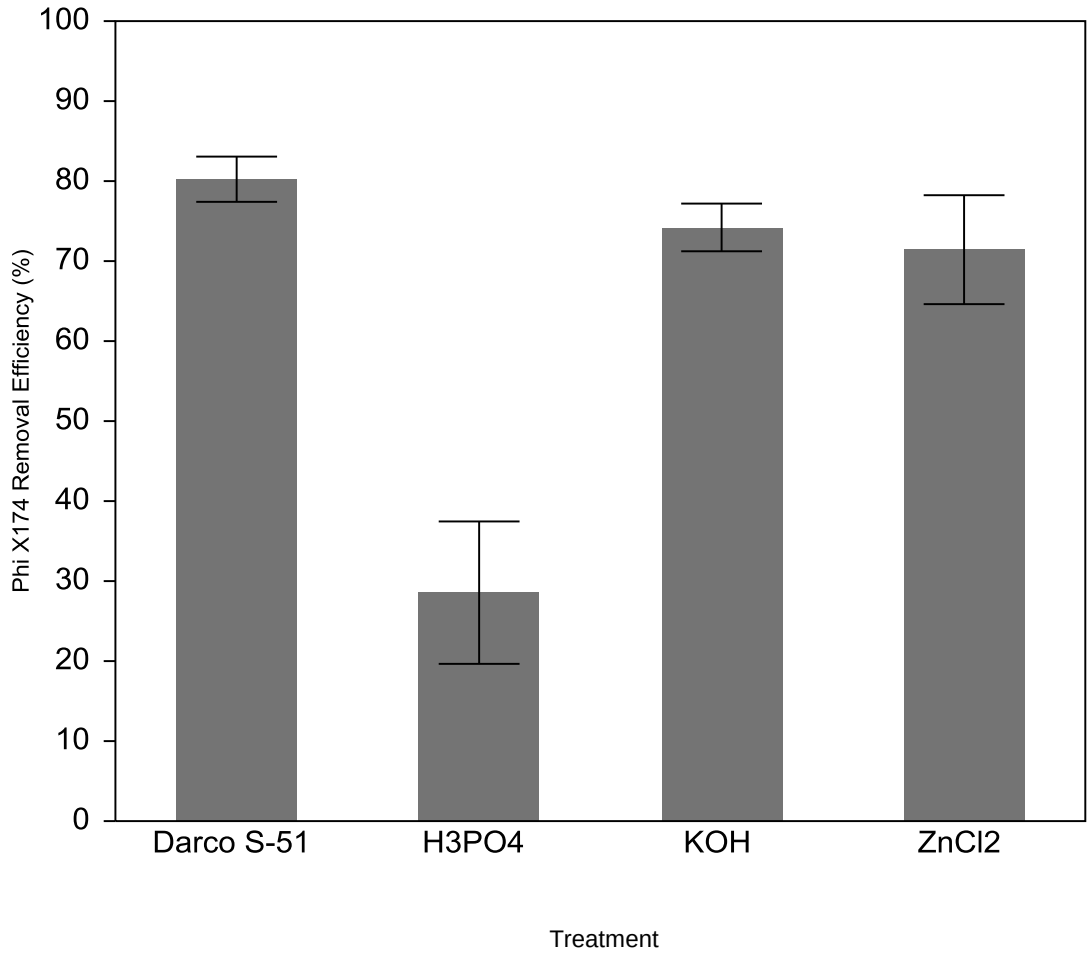

Figure 31: Effects of Activated Biochars on ΦX174 Levels in Surface Water. Error Bars Represent Standard Error of Three Replications

Removal efficiency of ΦX174 from surface water was similar to that of MS2 (Figure 31) with a few exceptions. The necessary seeding rate/baseline infectivity for ΦX174 was further reduced to 546.7 – 790 PFU/mL. At this rate, the efficiency of the H_3PO_4-activated biochar was increased to a mean removal of 28.56% (Table 22);

however, it was still the least effective treatment. Darco® S-51 displayed the greatest removal efficiency followed by the KOH and $ZnCl_2$ treatments.

Table 22: Means and Standard Deviations for Activated Biochar Effects on ΦX174 Levels (PFU/mL) in Surface Water

Level	N	Mean	Std Dev	Std Err Mean	Lower 95%	Upper 95%
Darco S-51	3	80.24	4.90	2.83	68.07	92.40
H_3PO_4	3	28.56	15.42	8.90	-9.74	66.85
KOH	3	74.21	5.16	2.98	61.38	87.04
$ZnCl_2$	3	71.43	11.79	6.81	42.14	100.72

As was the case with MS2, statistical delineation was possible only for the H_3PO_4-activated biochar (Table 23).

Table 23: Student's t-test for Activated Biochar Effects on ΦX174 Levels (PFU/mL) in Surface Water (α: 0.05)

Level	- Level	Difference	Std Err Dif	Lower CL	Upper CL	p-Value
Darco S-51	H_3PO_4	51.68	8.44	32.22	71.14	0.0003
KOH	H_3PO_4	45.65	8.44	26.19	65.11	0.0006
$ZnCl_2$	H_3PO_4	42.87	8.44	23.41	62.33	0.0010
Darco S-51	$ZnCl_2$	8.81	8.44	-10.65	28.27	0.3272
Darco S-51	KOH	6.03	8.44	-13.43	25.48	0.4954
KOH	$ZnCl_2$	2.78	8.44	-16.68	22.24	0.7503

Also, while the KOH-activated biochar was numerically less effective than the $ZnCl_2$-activated biochar in MS2 removal from surface water, the KOH treatment proved to be numerically more efficient that the $ZnCl_2$ treatment when used for removal of ΦX174 from surface water.

3.5.5 Effects of Activated Biochars on MS2 Levels in Groundwater

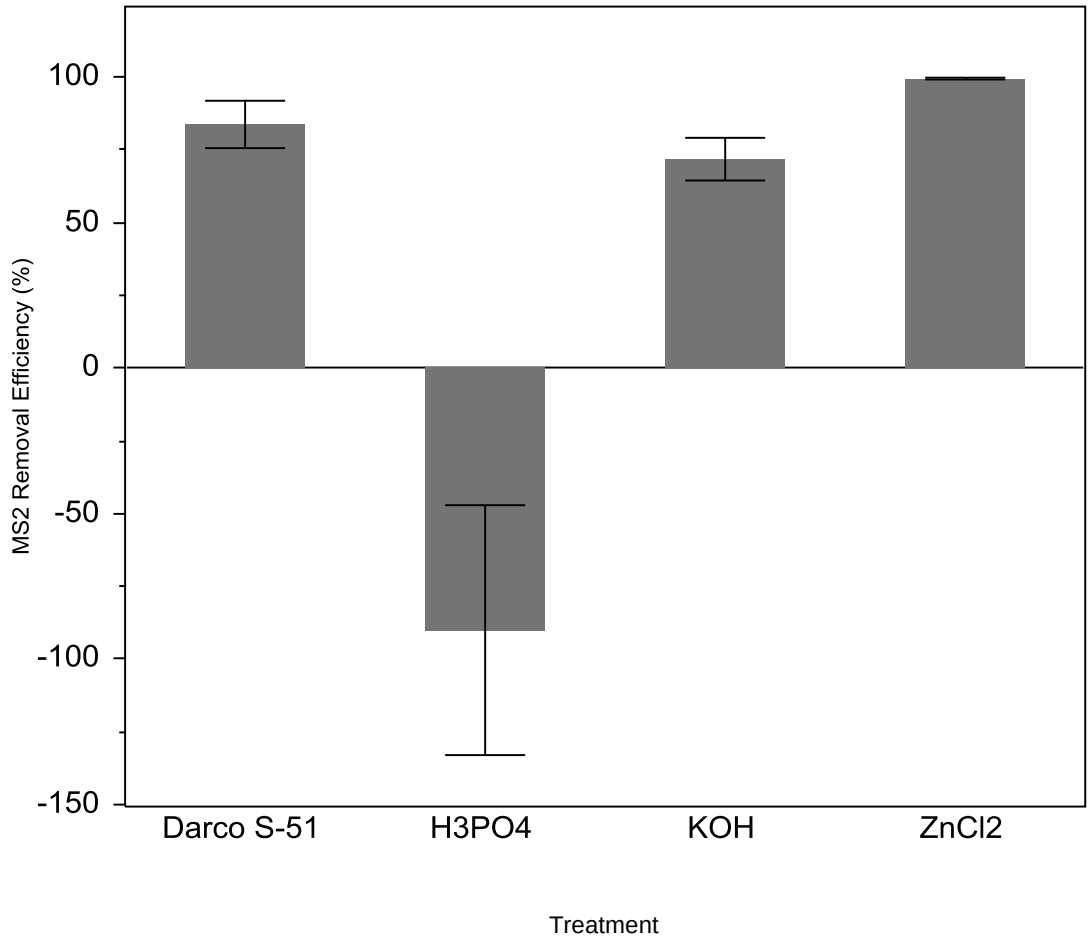

Figure 32: Effects of Activated Biochars on MS2 Levels in Groundwater. Error Bars Represent Standard Error of Three Replications

The results of the groundwater MS2 batch trials can be seen in Figure 32. Again, it is apparent in Figure 32 that the H_3PO_4-activated biochar was least effective in MS2 removal. In fact, the mean removal efficiency was actually a negative value (Table 24), suggesting that, in this instance, H_3PO_4-activated biochar actually appeared to *enhance* MS2 infectivity at a seeding rate ranging from $8.33 \times 10^8 – 3.35 \times 10^9$ PFU/mL.

Table 24: Means and Standard Deviations for Activated Biochar Effects on MS2 Levels (PFU/mL) in Groundwater

Batch	N	Mean	Std Dev	Std Err Mean	Lower 95%	Upper 95%
Darco S-51	3	83.75	14.10	8.14	48.74	118.77
H_3PO_4	3	-90.10	74.40	42.95	-274.91	94.71
KOH	3	71.81	12.70	7.33	40.26	103.35
$ZnCl_2$	3	99.50	0.55	0.32	98.15	100.86

As seen in Table 24, $ZnCl_2$-activated biochar was, by far, the most effective at 99.5% removal efficiency. Despite this fact, the $ZnCl_2$ treatment could not be statistically separated from the other treatments (Table 25). Again, the H_3PO_4-activated biochar was not only the least effective but also the only treatment that could be statistically separated.

Table 25: Student's t-test for Activated Biochar Effects on MS2 Levels (PFU/mL) in Groundwater (α: 0.05)

Level	- Level	Difference	Std Err Dif	Lower CL	Upper CL	p-Value
$ZnCl_2$	H_3PO_4	189.60	31.35	117.32	261.89	0.0003
Darco S-51	H_3PO_4	173.85	31.35	101.57	246.13	0.0005
KOH	H_3PO_4	161.91	31.35	89.63	234.19	0.0009
$ZnCl_2$	KOH	27.70	31.35	-44.59	99.98	0.4027
$ZnCl_2$	Darco S-51	15.75	31.35	-56.53	88.04	0.6288
Darco S-51	KOH	11.94	31.35	-60.34	84.23	0.7131

3.5.6 Effects of Activated Biochars on ΦX174 Levels in Groundwater

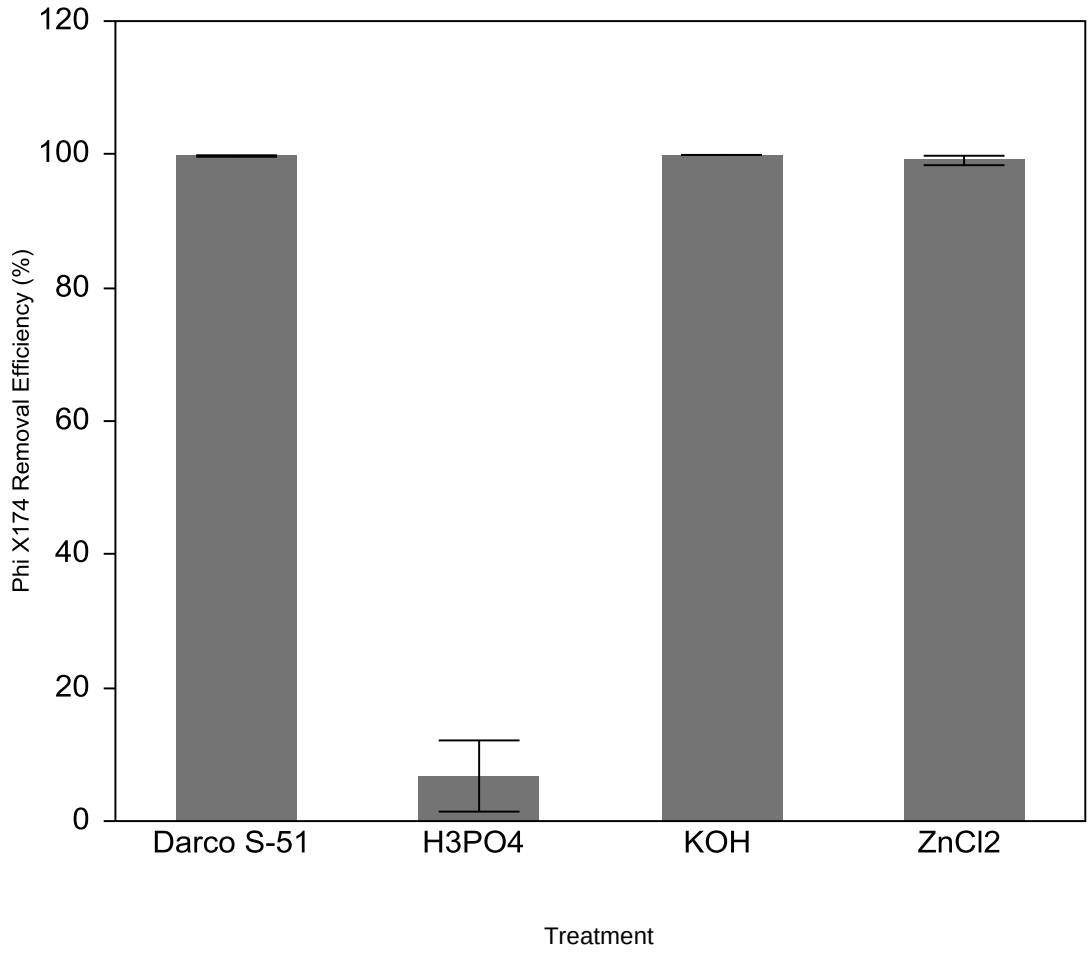

Figure 33: Effects of Activated Biochars on ΦX174 Levels in Groundwater. Error Bars Represent Standard Error of Three Replications

At a drastically reduced seeding rate, as compared to the MS2/groundwater rate of just 8,300 – 19,533 PFU/mL, most treatments were approaching 100% efficiency with the exception of the H_3PO_4-activated biochar (Figure 33) which had a mean ΦX174 removal efficiency of 6.76% (Table 26). The KOH-activated biochar exhibited the greatest efficiency at mean of 99.92% (Table 26), however both the $ZnCl_2$-activated

biochar and the Darco® S-51 were also above 99% making statistical separation of these three PACs impossible in this treatment (Table 27).

Table 26: Means and Standard Deviations for Activated Biochar Effects on ΦX174 Levels (PFU/mL) in Groundwater

Batch	N	Mean	Std Dev	Std Err Mean	Lower 95%	Upper 95%
Darco S-51	3	99.77	0.19	0.11	99.29	100.24
H_3PO_4	3	6.76	9.25	5.34	-16.22	29.75
KOH	3	99.92	0.02	0.01	99.89	99.96
$ZnCl_2$	3	99.10	1.23	0.71	96.05	102.15

Table 27: Student's t-test for Activated Biochar Effects on ΦX174 Levels (PFU/mL) in Groundwater (α: 0.05)

Level	- Level	Difference	Std Err Dif	Lower CL	Upper CL	p-Value
KOH	H_3PO_4	93.16	3.81	84.37	101.95	<.0001
Darco S-51	H_3PO_4	93.00	3.81	84.22	101.79	<.0001
$ZnCl_2$	H_3PO_4	92.33	3.81	83.55	101.12	<.0001
KOH	$ZnCl_2$	0.83	3.81	-7.96	9.61	0.8337
Darco S-51	$ZnCl_2$	0.67	3.81	-8.12	9.46	0.8648
KOH	Darco S-51	0.16	3.81	-8.63	8.94	0.9682

3.6 Mode of Inactivation

Bacteriophage levels in the post-seeded treatment extracts can be seen in Figure 34. Again, MS2 removal efficiency was used to measure the level of inactivation posed by potential chemical interactions of activated biochar extracts. A box-plot is used in Figure 34, as opposed to the bar graphs of other batch assays, to illustrate not only the level of variance among the individual treatment results, but also the overlap of all treatments. Additionally, use of the box-plot allows for clear illustration of treatment efficiencies above and below the baseline batch, which would be represented by the

zero-percent removal efficiency line. As seen in Figure 34, the zero-percent removal line is included within the statistical range of all treatments.

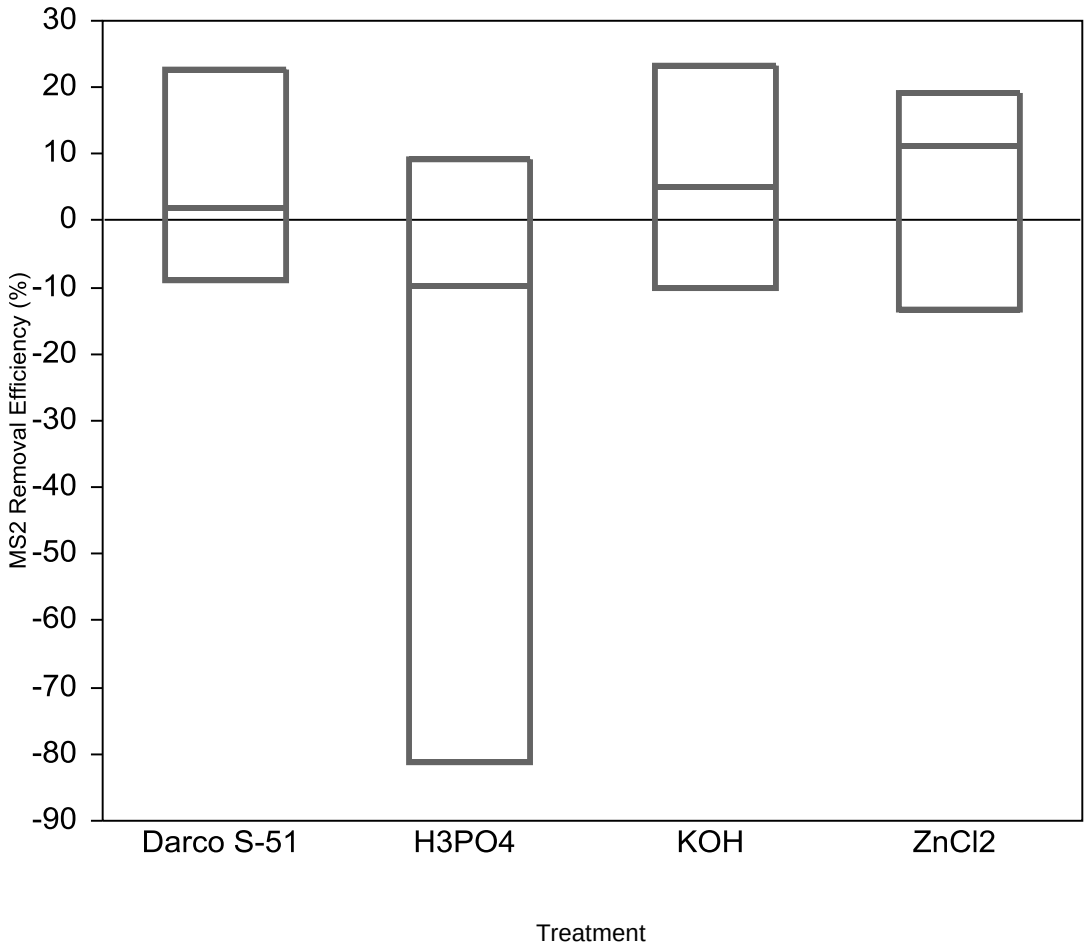

Figure 34: Effects of PAC Extracts on MS2 Levels. Error Bars Represent Standard Error of Three Replications

The extract having the most profound effects on MS2 levels was the H_3PO_4-activated biochar extract, with a mean of -27.22% removal efficiency (Table 28). The H_3PO_4-activated biochar extract also exhibited the greatest variance (Table 28).

Table 28: Means and Standard Deviations for PAC Extract Effects on MS2 Levels (PFU/mL)

Extract	N	Mean	Std Dev	Std Err Mean	Lower 95%	Upper 95%
Darco S-51	3	5.31	16.11	9.30	-34.72	45.34
H_3PO_4	3	-27.22	47.59	27.48	-145.45	91.00
KOH	3	6.16	16.63	9.60	-35.16	47.48
$ZnCl_2$	3	5.75	16.98	9.80	-36.43	47.93

Despite the relative effects of the H_3PO_4-activated biochar extract, statistical separation of PAC extracts was not possible (Table 29). Additionally, the zero-percent efficiency line, or baseline level, was within the 95% confidence intervals of all extracts (Table 28).

Table 15: Student's t-test for PAC Extract Effects on MS2 Levels (PFU/mL) (α: 0.05)

Level	- Level	Difference	Std Err Dif	Lower CL	Upper CL	p-Value
KOH	H_3PO_4	33.39	22.69	-18.94	85.71	0.1794
$ZnCl_2$	H_3PO_4	32.97	22.69	-19.35	85.30	0.1843
Darco S-51	H_3PO_4	32.54	22.69	-19.79	84.86	0.1895
KOH	Darco S-51	0.85	22.69	-51.48	53.18	0.9710
$ZnCl_2$	Darco S-51	0.44	22.69	-51.89	52.76	0.9851
KOH	$ZnCl_2$	0.41	22.69	-51.91	52.74	0.9859

The effects of the respective PACs on the groundwater solution pH can be seen in Table 30.

Table 30: Effects of PACs on Groundwater Solution pH

	Activation Treatment			
pH Value	**KOH**	**$ZnCl_2$**	**Darco S-51**	**H_3PO_4**
Mean of 3 Reps	8.63	8.24	8.47	7.897
Std. Dev. Of Mean	0.03	0.02	0.050	0.042
Change in pH	0.14	-0.25	-0.023	-0.590

The initial pH of the groundwater sample was determined to be 8.49, at the time of the pH effect tests. As seen in Table 30, all PACs had an acidifying effect on the groundwater solution pH, with exception of the KOH-activated biochar. The KOH-activated biochar elevated the pH by 0.14 units, while all others decreased solution pH. The H_3PO_4-activated biochar had the greatest effect, lowering the pH by 0.59 units; while the Darco® S-51 had the least significant effects, lowering the pH by only 0.023 units.

4. DISCUSSION

4.1 Biochar Activation

Currently, the process of producing activated carbon is not fully understood. Though the conditions may be optimized, to some degree, to obtain activated carbons with desired properties, all governing processes/reactions are yet to be completely realized. The chemicals used in this study for activation (KOH, $ZnCl_2$, and H_3PO_4) produced PACs of varying properties and with varying yield. The KOH-activated biochar yielded a mean heat treatment recovery of 61.4%. This is in contrast with the $ZnCl_2$ and H_3PO_4 treatments, both of which returned ~30% after heat treatment. Azargohar and Dalai reported (2008) that yield decreases as activation temperature increases. Additionally, the authors stated that the same effect could be seen with increases in chemical to biochar ratio and nitrogen flow rate, at higher temperatures. Furthermore, Azargohar and Dalai attempted to optimize the activation of biochar with KOH to reach both desired yield and BET surface area which they deemed to be ≥70% and ≥700 m^2/g, respectively. Given those goals, the authors determined the optimum activation model to be as follows: temperature = 680 °C, KOH:biochar ratio = 1.23, and N_2 flow rate = 240 mL/min. Under these conditions, they developed a PAC with a BET surface area of 836 m^2/g and a yield of 78%. The activation parameters of *this* study, however, were not designed to maximize yield or surface area but rather to create porosity within the PACs that would be capable of sorption of viral particles. In so

doing, total surface area and yield would be compromised. The maximum temperature used in this study exceeded the model of Azargohar and Dalai (2008) by 145 °C, the ratio of KOH:biochar by 0.77, and the N_2 flow rate by 60 mL/min; yet, the yield of KOH-activated biochar, in a one-trial maximum, was only ~9% less than the optimum model yield and possessed a surface area of almost 1500 m^2/g (discussed below), almost double the value achieved by the optimum model. It should be noted, however, that activated carbon research has only recently included the use of biochars as precursors. Biochars differ from typical precursors of activated carbon in that they are already carbonized. So, while the differences in treatment yields can be seen in both this and other studies, more investigation will be required using biochar as a precursor for the production of activated carbons in order to definitively correlate this phenomenon.

4.2 Biochar/PAC Characterization

Not only did the activation process have a profound effect on the properties of the biochar precursor, but marked differences were also seen amongst the various chemical treatments. Total surface area increases were substantial, but again, varied greatly amongst treatments. Prior to activation, the biochar exhibited a total surface area, as measured by BET, of only 3.64 m^2/g. This value was expanded to over 611 m^2/g in the $ZnCl_2$ treatment, 703 m^2/g in the H_3PO_4 treatment, and almost 1500 m^2/g in the KOH treatment, all of which were greater than the Darco® S-51 PAC (540.9 m^2/g). This is promising as it confirms the viability of biochar as a precursor to the formation of high-surface area PACs. Additionally, it suggests the conditions were more conducive

to the production of PACs of considerable surface area when compared with the industry carbon: Darco® S-51. The results of the BET analysis can be visually realized through inspection of the images generated by SEM. Considerable differences can be seen when comparing the non-activated biochar to all other treatments. The non-activated biochar has a flat, smooth, planar surface in all images. This is in stark contrast, particularly with the KOH-activated biochar, to the activated biochars across all treatments. This contrast was also witnessed by Uçar et al. (2009). In that study, the authors activated pomegranate seeds with $ZnCl_2$ and, for comparison, produced a biochar in the absence of $ZnCl_2$. The biochars produced in this study were determined to have a BET surface area of 2.63 and 2.92 m^2/g (carbonization temperature of 600 and 800 °C, respectively) and were regarded as having little, as indicated by SEM, significant surface pore structures as compared with the activated treatments.

Because the properties of activated carbons vary greatly depending on precursor, method of activation, ratio of activation method to precursor, maximum temperature, ramp rate, duration, gas flow, etc. (Azargohar and Dalai, 2006; Azargohar and Dalai, 2008; Castro et al., 2000; de D. López-González et al., 1980; Diao et al., 2002; Girgis et al., 1994; Girgis et al., 2002; Ioannidou and Zabaniotou, 2007; Molina-Sabio and Rodríguez-Reinoso, 2004; Olivares-Marín et al., 2006; Tan et al., 2008; Uçar et al., 2009), this study cannot definitively state that the parameters used herein were optimal for the formation of maximum surface area PACs within all treatments. Possibly, KOH is the most suitable chemical agent for activation of a biochar, or perhaps the most suitable agent for the activation parameters used in this study. These things remain

unclear and perhaps, due to the sheer number of combinations/variability among precursors and activation parameters, they always will. We can definitively say, however, that the process greatly enhanced the surface area characteristics amongst all treatments, as they pertain to our objectives, and that considerable variability amongst the chemical treatments can readily be seen.

This variability can also be seen in the results of the elemental analysis, as determined by a combination of Kjeldahl digest and ICP-MS analysis (Table 2). Percent carbon in the biochar prior to activation was 54.23%. This proportion was increased, through activation, in all treatments with the exception of the H_3PO_4 treatment. The most significant increase in % C was seen in the $ZnCl_2$-activated biochar, having a mean value of 72.09% C. This relative increase in C was also seen by Uçar et al. (2009); however, the precursor used in that study was not carbonized prior to activation.

The most notable observations of the elemental analysis were, as compared to the non-activated biochar, the reduction in K amongst all treatments, the increase in Zn in the $ZnCl_2$ treatment, and the increase in P and all basic cations in the H_3PO_4 treatment. The reduction in K can likely be explained by interactions with HCl and consequent dissolution from solution, as mentioned above. Obviously, the quantity of Zn in the $ZnCl_2$-activated biochar can be explained by the treatment. The more pressing issue would be the possibility of losing that Zn to solution while applying as a method of water purification. The total concentration of Zn in this treatment was 2359 mg/kg. It is therefore unlikely that sufficient quantities of Zn could be released so as to be detrimental, however, a comprehensive study analyzing the leachate of $ZnCl_2$-activated

biochar-treated waters would be necessary to fully determine what, if any, were the risks. The increase in P in the H_3PO_4 treatment can be attributed to the treatment itself. The more significant issue might be the fate of that P and potential complexes it may have formed. Those complexes might then explain the relative abundances of the basic cations found in this sample (K, Ca, Mg, and Na). Possibly, and perhaps likely, these cations interacted with PO_4^{3-} in the sample to form various phosphate complexes, all of which would be aided by the extreme heat and likely would have formed insoluble structures due to the extreme heating conditions. This occurrence would explain the presence of high mass materials seen in the backscattered electron SEM images. Presence of such high mass/high density compounds would increase the bulk density of a PAC; and, thus, it would be no surprise to learn the H_3PO_4-activated biochar exhibited the greatest bulk density amongst the PACs used in this study.

4.3 Surface Water and Groundwater Characterization

The results of the environmental water characterization seen in section 3.1 were not unexpected. Notably, the surface water sample, taken from Wolf Pen Creek, was much higher (over 4x's) in organic carbon and dissolved organic nitrogen (20x's) as well as total nitrogen. These differences are also reflected in nitrate- and ammonia-nitrogen as well as phosphate-phosphorous. The mean values of all anions and cations were significantly greater in the surface water sample as was the conductivity (2x's groundwater conductivity). The latter can conveniently be attributed to total Na^+ and Cl^- present in the surface water sample. All of this was, of course, to be expected as Wolf

Pen Creek is a surface water body located in a highly urbanized area. The groundwater sample, however, was pumped from the Carrizo-Wilcox Simsboro Sands aquifer which supplies the local communities and is known to be a fairly pristine aquifer, with exception of the Na^+ content. Additionally, surface water sample was determined to have an *E. coli* concentration of 300 colony forming units (CFU)/100 mL. This concentration is higher than the acceptable standard (126 CFU/100 ml) as defined by the Texas Commission on Environmental Quality (TCEQ). The relevance in characterization of the water sample quality is, of course, tied directly to potential sorption of target viral particles within the water matrix. Thus, as the surface water sample is markedly higher in almost all measurable categories, it would be expected that virus removal efficiency might be lower within these samples.

4.4 Batch Analyses

As no indigenous particles were detected in the unseeded biochar batch, it was determined that the material contained no inherent MS2 particles and was consequently discontinued. In its non-activated state, the biochar was entirely ineffective in removing MS2 particles from PBS. In fact, there was no statistical difference between the biochar treated batch and the baseline. If using total surface area as a barometer for viral sorption potential, the lack of effect presented by the non-activated char would come as no surprise. By this measure, it would be expected that the KOH-activated biochar would have the greatest sorption and, in the PBS matrix, this was the case.

With an MS2 removal efficiency of over 98% at a particle concentration ranging from 2.5 – 6.25 x 10^9 PFU/mL, the KOH-activated biochar exceeded all other treatments by at least 10% efficiency and an order of magnitude in viral particle reduction in the PBS matrix. This resulted in statistical delineation of the KOH treatment, with exception of the $ZnCl_2$ treatment. The $ZnCl_2$ treatment was not significantly different than the Darco® S-51. The H_3PO_4 treatment, due to its low removal efficiency, was significantly lower when compared with all treatments. Consequently, sorption efficiency cannot be solely attribute to surface area value as both the Darco® S-51 (surface area = 540.87 m^2/g) and the $ZnCl_2$-activated biochar (surface area = 611.15 m^2/g) exhibited greater removal efficiency than the H_3PO_4-activated biochar (surface area = 703.78 m^2/g).

As previously stated Seo et al. (1996), used a complex system combining a PAC with microfiltration to remove bacteriophage Qβ, very similar to MS2, from a synthetic secondary effluent. The authors were able to achieve a removal efficiency of 99.99%, however, the concentration of PAC used to attain that value was 550 mg/L (or 110 mg/200 mL). Additionally, the matrix used in this assay lacked a number of constituents used to produce the synthetic effluent, notably: humin, lignin, tannin, and Arabic gum. At a sorbent concentration of 52 mg/200 mL (more comparable to the MS2/PBS batch of this study), coliphage Qβ was reduced from 2.4 x 10^7 to 2.2 x 10^4 PFU/mL, essentially a reduction of 2.4 x 10^7 PFU/mL. At a comparable concentration, the KOH-activated biochar used in this study was able to reduce the MS2 concentration in PBS from a mean of 4.18 x 10^9 to 5.01 x 10^7 PFU/mL, an effective reduction of 4.13 x 10^9 PFU/mL. Not

only was the KOH-activated biochar able to demonstrate a tremendous increase in total reduction, as compared to the aforementioned study, it was able to do so without the additional treatment effects present in the complex filtration system used by Seo et al.

It was hypothesized that the surface water matrix would provide some challenge to virus removal efficiency due to the comparably high level of background within the sample. It was expected that a great deal of competitive inhibition for sorption sites would therefore be present. Gerba et al. (1975) examined the effects of organics in secondary effluent on the adsorption of poliovirus. That work confirmed the competition by soluble organics for sorption sites. In our study, both MS2 and ΦX174 removal efficiencies from surface water were at or below 80% in all treatments, a significant reduction compared to efficiencies seen in PBS and groundwater matrices, despite having reduced baseline infectivity ranges of 8,400 – 15,133 and 546.6 – 790 PFU/mL, respectively. Because Gerba et al. (1975) did not characterize the effluent used in their study, direct comparisons between that matrix and the surface water used in this study cannot be definitively stated; though, it is possible they were somewhat similar in quality. Due to the level of treatment a secondary effluent would have received, it might be possible to assume the quality of such a sample to be higher than that of raw surface water. In any case, the PAC used by Gerba et al. (1975) was able to remove only 57% of poliovirus particles in a 50% dilution of effluent (tap water used as diluent) and a seeding rate of 6.5×10^3 PFU/mL (PAC concentration unknown). More effective removal efficiencies were, in that study, realized at pH values <4.5. The authors attributed this to the increase in positive surface charges seen in poliovirus at

lower pH values. Powdered activated carbons produced from biochar in the present study were, with the exception of the H_3PO_4-activated biochar, able to surpass this removal efficiency. As seen with the $ZnCl_2$-activated biochar, MS2 removal efficiency from 75% surface water had a mean value of 75.65% at seeding rates ranging from 8.4 x 10^3 – 1.51 x 10^4 PFU/mL.

In contrast, the groundwater matrix batches which, when compared to the surface water, were comparably pristine and did not seem to provide the substantial competitive inhibition. In the case of MS2 removal from groundwater, the $ZnCl_2$-activated biochar removed a mean of 99.5% of particles at a baseline concentration ranging from 8.33 x 10^8 – 3.35 x 10^9 PFU/mL. Because removal efficiencies were greater, or at least similar (KOH, Darco® S-51), in a groundwater matrix despite having an increased seeding concentration of several orders of magnitude, suspicions regarding the influence of water quality on the removal efficiency of any sorbent product are, again, confirmed. Similar effects were seen in the removal efficiency of ΦX174 from groundwater. All treatments, with exception of the H_3PO_4-activated biochar, exhibited mean removal efficiencies greater than 99%, again at an increased baseline concentration (8,300 – 19,533 PFU/mL). As with all other batches, with exception of MS2 removal from PBS, the statistical separation of treatment effects was possible only with the H_3PO_4-activated biochar.

It should be noted that the activated carbons used by both Seo et al. (1996) and Gerba et al. (1975) were industrially manufactured by large producers of activated carbon and other products. In both cases, coal, a fossil fuel requiring millennia to form

and having value not related to activated carbon, was used as the production precursor. This is in contrast to the precursor used for PAC production in this study, biochar, a byproduct of an energy conversion process that may prove to be of substantial value regarding the need for cleaner, greener energies.

Prior to this study, it was thought that variances in sorption efficiencies due to biochar activation treatments, virus type, and matrix quality would be present. Seemingly, those variances were realized. Chemical activation treatment appeared to have a profound effect on surface area, as seen in the BET analysis. The only batch in which the treatment with the greatest reduction efficiency could be statistically separated from all other treatments was the PBS/MS2 batch. In this experiment, the treatment with the greatest surface area (KOH-activated) exhibited the greatest removal efficiency. Because the H_3PO_4-activated biochar was not the second most effective sorbent, we cannot statistically, or numerically, say that surface area is *the* PAC quality governing sorption efficiency. The H_3PO_4-activated biochar, however, is a curious case. Not only was the removal efficiency of this treatment not indicative of its surface area, the efficiency was so low that, in the case of MS2 removal from groundwater, it appeared to actually *enhance* viral infectivity to a significant degree. This phenomenon was consequently further examined by statistically comparing the mean PFU/mL concentrations of the baseline and H_3PO_4-activated biochar filtrates in the MS2/groundwater batches. No statistical separation of the MS2 concentration in these filtrates could be made (data not shown). Though it cannot be definitively said that H_3PO_4-activated biochar enhances infectivity, based on the results of this study, it can be

concluded that this treatment is much less effective in virus removal than the others. This occurrence may be explained by aforementioned formation of PO_4^{3-} complexes, evidenced by both the elemental and SEM analyses. These complexes are of relatively high mass/density when compared with the respective carbon matrix. Such high quantities of this material would give the H_3PO_4-activated biochar a greater bulk density when compared to the other treatments. Because all PACs were added to the batch mixtures based on mass (50 mg) and assuming the H_3PO_4-activated biochar possessed the greatest bulk density value, the volume of added H_3PO_4-activated biochar would be the least significant, i.e. it would present the lowest concentration of sorbent and least potential surface area for each sorption batch. Though the bulk density of all PACs was not determined, it was extremely clear upon visual inspection that while a mass of 50 mg of each PAC may have been a standardized value, the volume of 50 mg of each PAC could be highly variable. The KOH-activated biochar, for example, clearly displayed the lowest bulk density. So, while the KOH treatment appeared to yield the lowest recovery from the activation process, this recovery was based on mass not volume. Therefore, when added as a sorption treatment, the KOH-activated biochar was added in the greatest volume/concentration. These respective differences in bulk density may explain the variance in virus removal efficiency, particularly in the case of H_3PO_4-activated biochar.

In addition to chemical treatment, virus type and water quality played a significant role in removal efficiency. These factors cannot be understated as they will have direct impacts on the practical application of this research. As there are many types

of viruses affecting many groups of hosts, we would expect viruses to exhibit a vast array of properties. One such property is the viral surface isoelectric point (IEP). The two phages used in this study were chosen, as mentioned, not only for their ease in propagation and quantification, but for their respective differences, thus allowing for the testing of these PAC products on viruses of varying properties. Given that MS2 has an IEP of 3.9, it should be expected to exhibit a much more significant charge at, or near, neutral pH than will ΦX174 (IEP 6.6). Due to this fact, we might then assume that MS2 will be removed in greater abundances at, or near, neutral pH than will ΦX174, if significance of surface charge is the determining factor. Add to this equation the effects of surface water quality on virus removal efficiency and we could then deduce that the greatest quantity of viral particles removed *should* be found in the removal of MS2 from the most pristine matrix: PBS. Conversely, we would expect to find that the virus removed in the lowest abundance should be found in the removal of ΦX174 from the least pristine matrix: surface water. As seen in sections 3.5.2 and 3.5.4, respectively, this was exactly the case. Based on this evidence, it is clear that both the characteristics of the matrix and the virus will greatly influence the efficacy of this type of water treatment. Gerba et al. (1975) found that viral sorption efficiencies were enhanced at lower pH values. The H_3PO_4-activated biochar had the greatest effect on solution pH (Table 30). However, the authors of that study noted that removal efficiencies were greatest at pH values <4.5, below the IEP of the virus used in that study. The authors also noted that activated carbons become negatively charged above pH 2.8. Therefore, in that instance, the solution pH was below the IEP of the target virus, creating positive

surface charges, but not low enough to result in a positively charged sorbent. In the current study, the H_3PO_4-activated biochar lowered the solution pH by a much greater degree than did the other treatments, creating a sorbent with less overall negative charge. But, because pH did not reach a level below the IEP of either MS2 or ΦX174, the result was a negative effect on the electrostatic potential of the H_3PO_4-activated biochar to remove viral particles.

All of the aforementioned conclusions/assumptions are based on the physical sorption and consequent removal of viral particles from aqueous solution. It was therefore prudent to attempt to eliminate the possibility of chemical inactivation of viral particles in solution by testing the relative "removal efficiency" of an extract derived from biochar/PAC solutions. In Figure 34, the "zero-percent removal line" can be seen dissecting all treatment box plots. Additionally, the 95% confidence interval of all treatments (Table 29) includes a value of zero. Because of this, the baseline infectivity level, or 100% infectivity, cannot be statistically delineated from the any of the treatment extract effects. Consequently, it cannot be said that the chemical extract of any treatment, in this study, had a significant effect on virus viability/infectivity. With this possibility excluded, we may assume that viral sorption by the PAC treatments is the most likely cause of for the reduction in viral particles seen across the various experimental treatments. It should be noted that not only were the treatment extract effects not statistically separable from the baseline level, they were also statistically inseparable from one another (Table 30).

5. CONCLUSIONS

The above results from this study support the following conclusions:

1. Biochar derived from the pyrolysis of corn stover is, in its non-activated state, not suitable as a viral sorbent. This determination is based on the efficiency of non-activated biochar to remove MS2 from a 'pristine water' matrix: PBS.

2. The activation parameters selected for creating a PAC, using biochar as a precursor, were, in most cases, appropriate. Parameters were chosen to target desired pore diameters. Because the PACs were highly effective in virus removal, the activation parameters should be considered appropriate. The one exception was the use of H_3PO_4 as an activating agent which encouraged the formation of various PO_4^{3-} complexes.

3. Through physical and chemical characterization of the biochar/PACs, we were able to determine the effects of and consequent differences of the various chemical activating agents. Accordingly, it might then be possible to select the appropriate agent for the desired application of the final product.

4. The efficiency of the PACs resulting from the activation of biochar is dependent on a number of variables. They include but are not limited to:

    a) Sorbent concentration: the range in visible bulk density of the PACs led to a varying range in sorbent concentration, as added on a mass basis.
    b) Water quality: the three matrices used in this study may be ranked as follows: PBS, groundwater, surface water. Predictably, the greatest quantities of particles were removed from the three matrices in the exact order of their water quality ranking: PBS, groundwater, surface water.
    c) Virus type: While the two phages used in this study had fairly similar morphologies, they had substantially different IEPs. This led to varying charge densities amongst the two viral strains and, therefore, to varying quantities with which they were sorbed to the PAC surface.
    d) PAC type: In this study, H_3PO_4 did not produce a desirable PAC as compared to other treatments. This would suggest that the parameters for activation are important not only for enhancing total surface area, but for creating desirable surface area characteristics conducive to sorption of target contaminants.

5. Removal efficiency of the PACs produced from biochar in this study appeared to be the result of physical sorption rather than chemical inactivation of treatment leachates.

Overwhelmingly, based on the results of this study, if the potential of pyrolysis is realized such that it becomes a staple of global energy production, activation of the co-product (biochar) might, along with process of pyrolysis, simultaneously address the global needs for clean, renewable energy and also potable water, free of viral contaminants.

REFERENCES

American Water Works Association W.E.F., American Public Health Association. 2005. Standard Methods for the Examination of Water and Wastewater, 21st Edition, Detection of Coliphages, American Public Health Association, Washington D.C.

Asadullah M., Rahman M.A., Ali M.M., Rahman M.S., Motin M.A., Sultan M.B., Alam M.R. 2007. Production of bio-oil from fixed bed pyrolysis of bagasse. Fuel 86:2514-2520.

Azargohar R., Dalai A.K. 2006. Biochar as a precursor of activated carbon . pp. 762 - 773. *In* J. D. McMillan, et al. (Eds.), Twenty-Seventh Symposium on Biotechnology for Fuels and Chemicals. Humana Press, Totowa, New Jersey.

Azargohar R., Dalai A.K. 2008. Steam and KOH activation of biochar: Experimental and modeling studies. Microporous and Mesoporous Materials 110:413-421.

Bitton G. 2005. Water and Wastewater Disinfection. pp. 173-210. *In* Wastewater Microbiology, John Wiley & Sons, Inc. Hoboken, New Jersey.

Bosch A. 1998. Human enteric viruses in the water environment: a Minireview. International Microbiology 1:191-196.

Castro J.B., Bonelli P.R., Cerrella E.G., Cukierman A.L. 2000. Phosphoric acid activation of agricultural residues and bagasse from sugar cane: Influence of the experimental conditions on adsorption characteristics of activated carbons. Industrial & Engineering Chemistry Research 39:4166-4172.

Cerny S. 1964. Introduction. pp. 1-9. *In* Active Carbon: Manufacture, Properties and Applications, Elsevier, New York, New York.

Chattopadhyay S., Puls R.W. 1999. Adsorption of bacteriophages on clay minerals. Environmental Science & Technology 33:3609-3614. DOI: 10.1021/es9811492.

Craun G., Craun M., Calderon R., Beach M. 2006. Waterborne outbreaks reported in the United States. Journal of Water and Health 4 Suppl 2:19-30.

de D. López-González J., Martínez-Vilchez F., Rodríguez-Reinoso F. 1980. Preparation and characterization of active carbons from olive stones. Carbon 18:413-418.

Diao Y., Walawender W.P., Fan L.T. 2002. Activated carbons prepared from phosphoric acid activation of grain sorghum. Bioresource Technology 81:45-52.

Elad Y., David D.R., Harel Y.M., Borenshtein M., Kalifa H.B., Silber A., Graber E.R. 2010. Induction of systemic resistance in plants by biochar, a soil-applied carbon sequestering agent. Phytopathology 100:913-921.

Gerba C.P., Sobsey M.D., Wallis C., Meinick J.L. 1975. Adsorption of poliovirus onto activated carbon in waste water. Environmental Science & Technology 9:727-731.

Girgis B.S., Khalil L.B., Tawfik T.A.M. 1994. Activated carbon from sugar cane bagasse by carbonization in the presence of inorganic acids. Journal of Chemical Technology & Biotechnology 61:87-92.

Girgis B.S., Yunis S.S., Soliman A.M. 2002. Characteristics of activated carbon from peanut hulls in relation to conditions of preparation. Materials Letters 57:164-172.

Golmohammadi R., Valegård K., Fridborg K., Liljas L. 1993. The refined structure of bacteriophage MS2 at 2·8 Å resolution. Journal of Molecular Biology 234:620-639.

Graber E., Meller Harel Y., Kolton M., Cytryn E., Silber A., Rav David D., Tsechansky L., Borenshtein M., Elad Y. 2010. Biochar impact on development and productivity of pepper and tomato grown in fertigated soilless media. Plant and Soil 337:481-496.

Havlin J.L., Soltanpour P.N. 1980. A nitric acid plant tissue digest method for use with inductively coupled plasma spectrometry 1. Communications in Soil Science and Plant Analysis 11:969-980.

International Committee on the Taxonomy of Viruses (ICTVdB). 2006. Enterobacteriophage ∅X174. Database available at http://ictvonline.org/virusTaxonomy.asp?version=2009&bhcp=1

Ilag L.L., McKenna R., Yadav M.P., BeMiller J.N., Incardona N.L., Rossmann M.G. 1994. Calcium ion-induced structural changes in bacteriophage ∅X174. Journal of Molecular Biology 244:291-300.

Ioannidou O., Zabaniotou A. 2007. Agricultural residues as precursors for activated carbon production--A review. Renewable and Sustainable Energy Reviews 11:1966-2005.

Laird D.A., Brown R.C., Amonette J.E., Lehmann J. 2009. Review of the pyrolysis platform for coproducing bio-oil and biochar. Biofuels, Bioproducts and Biorefining 3:547-562.

Laird D.A., Fleming P., Davis D.D., Horton R., Wang B., Karlen D.L. 2010. Impact of biochar amendments on the quality of a typical midwestern agricultural soil. Geoderma 158:443-449.

Lehmann J. 2007a. A handful of carbon. Nature 447:143-144.

Lehmann J. 2007b. Bio-energy in the black. Frontiers in Ecology and the Environment 5:381-387.

Lehmann J., Gaunt J., Rondon M. 2006. Bio-char sequestration in terrestrial ecosystems – A review. Mitigation and Adaptation Strategies for Global Change 11:395-419.

Liesch A.M.W., Sharon L.; Gaskin, Julia W.; Das, K.C. 2010. Impact of two different biochars on earthworm growth and survival. Annals of Environmental Science 4:1-9.

Major J., Rondon M., Molina D., Riha S., Lehmann J. 2010. Maize yield and nutrition during 4 years after biochar application to a Colombian savanna oxisol. Plant and Soil 333:117-128.

McGeehan S.L., Naylor D.V. 1988. Automated instrumental analysis of carbon and nitrogen in plant and soil samples 1. Communications in Soil Science and Plant Analysis 19:493-505.

McKenna R., Xia D., Willingmann P., Ilag L.L., Rossmann M.G. 1992. Structure determination of the bacteriophage ∅X174. Acta Crystallographica Section B 48:499-511. DOI: doi:10.1107/S0108768192001344.

Molina-Sabio M., Rodríguez-Reinoso F. 2004. Role of chemical activation in the development of carbon porosity. Colloids and Surfaces A: Physicochemical and Engineering Aspects 241:15-25.

Olivares-Marín M., Fernández-González C., Macías-García A., Gómez-Serrano V. 2006. Preparation of activated carbon from cherry stones by chemical activation with $ZnCl_2$. Applied Surface Science 252:5967-5971.

Overby L.R., Barlow G.H., Doi R.H., Jacob M., Spiegelman S. 1966. Comparison of two serologically distinct ribonucleic acid bacteriophages I. Properties of the viral particles. J. Bacteriol. 91:442-448.

Reynolds K.A., Mena K.D., Gerba C.P. 2008. Risk of waterborne illness via drinking water in the United States. pp. 117-158. *In* D. M. Whitacre (Ed.), Reviews of Environmental Contamination and Toxicology, Springer, New York, New York.

Rondon M., Lehmann J., Ramírez J., Hurtado M. 2007. Biological nitrogen fixation by common beans (*Phaseolus vulgaris* L.) increases with bio-char additions. Biology and Fertility of Soils 43:699-708.

Seo G.T., Suzuki Y., Ohgaki S. 1996. Biological powdered activated carbon (BPAC) microfiltration for wastewater reclamation and reuse. Desalination 106:39-45.

Tan I.A.W., Ahmad A.L., Hameed B.H. 2008. Optimization of preparation conditions for activated carbons from coconut husk using response surface methodology. Chemical Engineering Journal 137:462-470.

Texas Commission on Envrionmental Quality (TCEQ). 2011. Map of Water Systems under Water Use Restriction. Austin, Texas. Available at http://www.tceq.texas.gov/drinkingwater/trot/location.html

Uçar S., Erdem M., Tay T., Karagöz S. 2009. Preparation and characterization of activated carbon produced from pomegranate seeds by $ZnCl_2$ activation. Applied Surface Science 255:8890-8896.

United Nations Children's Fund (UNICEF). 2006. Water, sanitation and hygiene. pp. children and water: Global statistics. Available at http://www.unicef.org/wash/index_31600.html

United States Census Bureau. 2011. World population summary. Washington D.C.

United States Environmental Protection Agency (USEPA). 1993a. Method 353.2: Determination of nitrate-nitrate nitrogen by automated colorimetry. Washington D.C.

USEPA. 1993b. Method 350.1: Determination of ammonia nitrogen by semi-automated colorimetry. Washington D.C.

USEPA. 1993c. Method 365.1: Determination of phosphorous by semi-automated colorimetry. Washington D.C.

USEPA. 2002. Method 1603: *Escherichia coli* (*E. coli*) in water by membrane filtration using modified membrane-Thermotolerant *Escherichi coli* agar (Modified mTEC). Washington D.C.

USEPA. 2009. Final contaminant candidate list 3 microbes: PCCL to CCL process. Office of Water (Ed.). Washington D.C.

Van Zwieten L., Kimber S., Morris S., Chan K., Downie A., Rust J., Joseph S., Cowie A. 2010. Effects of biochar from slow pyrolysis of papermill waste on agronomic performance and soil fertility. Plant and Soil 327:235-246.

Verheijen F.G.A.J., S.; Bastos, A.C.; van der Velde, M.; and Diafas, I. 2009. Biochar application to soils - A critical scientific review of effects on soil properties, processes and functions. Office for the Official Publications of the European Communities, Luxembourg.

Yaman S. 2004. Pyrolysis of biomass to produce fuels and chemical feedstocks. Energy Conversion and Management 45:651-671.

VITA

James David Florey received his Bachelor of Science degree in Agronomy, with an emphasis on Soil Science, from Texas A&M University in 2009. He entered the Soil and Aquatic Microbiology program at Texas A&M University in September 2009 and received his Master of Science degree in May 2012. His research interests include environmental microbiology, virology, various environmental soil science applications, hydrogeology, and electron microscopy. He currently is employed as an Environmental Scientist by W&M Environmental Group and is actively pursuing licensure as a Professional Geoscientist (P.G.).

Mr. Florey may be reached at The Department of Soil and Crop Sciences of Texas A&M University, c/o Dr. Terry Gentry: Texas A&M Department of Soil and Crop Sciences, 370 Olsen Blvd. Mailstop #2474, College Station, TX 77843-2474. His email is JFlorey@ag.tamu.edu.